

ACOUSTICAL PARAMETERS

Franco Daniel Areco

Universidad Nacional de Tres de Febrero, Ingeniería de Sonido, Caseros, Buenos Aires, Argentina
email:francoareco53@gmail.com

Juan Martín Rucci

Universidad Nacional de Tres de Febrero, Ingeniería de Sonido, Caseros, Buenos Aires, Argentina
email:rucci45744@estudiantes.untref.edu.ar

Juan Almaraz

Universidad Nacional de Tres de Febrero, Ingeniería de Sonido, Caseros, Buenos Aires, Argentina
email:juan.almaraz097@gmail.com

Calquin Facundo Epullan

Universidad Nacional de Tres de Febrero, Ingeniería de Sonido, Caseros, Buenos Aires, Argentina
email:epullan44186@estudiantes.untref.edu.ar

This paper describes the procedures used to measure the acoustic parameters of the Soka Gakkai Peace Auditorium in the city of Buenos Aires. Monaural and binaural recordings were made using different types of microphones and loudspeakers. These recordings were processed using specialised software to obtain impulse responses and calculate various acoustic parameters, such as reverberation times, intelligibility and sound clarity. The measured room was found to be suitable for both spoken word, as it has good intelligibility but low clarity, and for music, as it facilitates the localisation of sources.

Keywords: Auditorio de la Paz, Soka Gakkai, acoustical parameters, auditory, impulse response

1. Introduction

Acoustic systems can be considered linear and time invariant and can therefore be characterised by their impulse responses. By measuring these impulse responses, a number of acoustic parameters can be obtained that help to understand and evaluate the behaviour of the enclosure.

There are objective and subjective acoustic parameters. The objective ones take into account the physical and technical aspects of sound, while the subjective ones are influenced by the auditory perception and integration process of the human being. In order to obtain a comprehensive evaluation of a room, an analysis of various acoustic parameters such as reverberation time, clarity and intelligibility is carried out. These parameters are compared with the recommendations established by different authors to determine the state of the room and propose possible solutions to improve its acoustics.

ISO 3382 [1] serves as a guide for the measurement of acoustic parameters. One of the common ways to measure reverberation time is by capturing an impulse response of the room, often obtained from a swept sinusoidal signal. These measurements not only allow anomalies to be detected and recommendations to be made, but can also validate computational designs and aid in the creation of an immersive acoustic environment.

A measurement is made in *Auditorio de la Paz Soka Gakkai* from Buenos Aires, Argentina. It hosts various lectures, seminars, courses, prayer meetings, religious ceremonies and meetings of Soka Gakkai members to practice and study Nichiren Buddhism. Occasionally, however, concerts are also held here. Overall, the auditorium serves as a meeting place for the Buddhist community. Here, a variety of acoustic parameters are studied. To obtain these measurements, different test signals and recording techniques are used, such as logarithmic sine sweeps, anechoic audios and specialised microphones. The aim is to obtain a detailed characterisation of the acoustic behaviour of the auditorium and to use this information to evaluate its sound quality and propose improvements if necessary.

2. State of the Art

Over an extended period, the acoustics of listening rooms have been investigated, leading to the proposal of acoustic parameters based on objective and subjective characteristics. Initially, W.C. Sabine introduced the reverberation time (RT60) in 1922 [2], which was followed by parameters such as the Early Decay Time (EDT) [3] and clarity parameters (C50 and C80) [4] to assess the intelligibility of speech and music. The Inter Aural Cross Correlation (IACC) binaural specification has also been proposed to measure the similarity between time-shifted musical signals [5]. Currently, more than 30 variables are available to characterise the acoustics of these rooms.

Even if two rooms have the same reverberation time, they can generate different auditory perceptions. Several studies have contributed to the improvement and expansion of existing parameters. Improved formulas for the calculation of reverberation time have been proposed, their optimal applicability in concerts has been explored and a value for the Just Noticeable Difference (JND) of RT has been established [6].

Recording the impulse response of a hall has become an essential tool for its characterisation. Methods such as the generation of impulse sounds by clapping, the explosion of a balloon [7] [8] [9] or the use of logarithmic sinusoidal sweeps [10] [11] simulate the impulse response. There is also commercial software that facilitates the calculation of various parameters by analysing this response. Examples of these are Aurora plugin [12] or EASERA [13].

In the context of Argentina, specific studies have been carried out in theatres and auditoriums such as the Teatro Colón [14], the Border Theatre in Buenos Aires [15], La Ballena Azul [16] and the Auditorio Juan Victoria in San Juan [17]. These studies contribute to a better understanding of the particular acoustic characteristics of these spaces.

The investigation into auditorium acoustics has resulted in the formulation of diverse parameters for their comprehensive characterization. Ranging from fundamental aspects such as reverberation time to more nuanced parameters, continuous endeavors have been undertaken to enhance, expand, and fine-tune the comprehension of these acoustic features. This evolution encompasses the incorporation of impulse response analysis facilitated by specialized software. Furthermore, the enrichment of acoustic knowledge has been achieved through localized studies, particularly those concentrating on theaters and auditoriums in Argentina.

3. Theoretical Framework

3.1 Reverberation Time (RT)

The Reverberation Time (*RT*) is defined as the period required for the sound intensity to decrease by 60 decibels (dB) after the interruption of the sound source. This measurement standard, which uses a 60 dB reduction as a reference, provides an objective metric for evaluating the acoustic characteristics of a room. The *RT* is essential for the characterization of room acoustics as it influences the sound quality in various applications such as concert halls, recording studios, and classrooms.

To obtain the Reverberation Time T_{30} and T_{20} , dynamic ranges less than 60 dB are considered and extrapolated from T_{60} . T_{30} is defined as the time it takes for the sound decay curve to drop from -5

dB to -35 dB below the initial level, while T_{20} is defined as the time it takes to drop from -5 dB to -25 dB.

The early decay time (EDT) shall be evaluated from the slope of the integrated impulse response curves (as the conventional reverberation time). The slope of the decay curve should be determined from the slope of the best-fit linear regression line of the initial 10 dB (between 0 dB and -10 dB) of the decay.

These reverberation time parameters provide a detailed understanding of how sound behaves in a space and are essential in the design and evaluation of acoustical environments for various applications.

It is important to note that when the sound decay is linear, i.e. when the decay curve of the sound intensity follows a constant path, the values of T_{60} , T_{20} and T_{30} are identical. This means that if one knows the value of T_{60} in a given room, one can accurately infer the values of T_{20} and T_{30} , which greatly simplifies the process of acoustic measurement and analysis. This phenomenon is clearly reflected in Figure 1, where the equality of these parameters is observed when the linear decay condition is met.

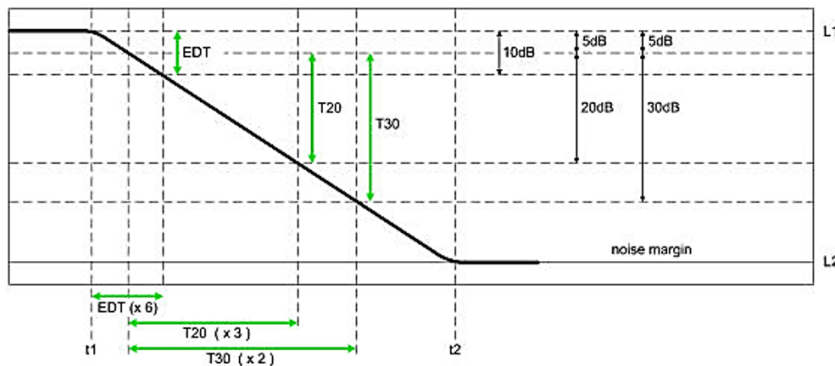


Figure 1: Diagram illustrating the comparison of EDT, T_{20} , and T_{30} .

3.2 Clarity parameters (C_{50} and C_{80})

International standard ISO 3382-1 defines C_{50} and C_{80} as the ratio of the sound energy arriving within a given time interval (50 or 80 ms, respectively) to the energy arriving after that interval. C_{50} is often used as an indicator of speech clarity in a hall, whilst C_{80} is used as an indicator of music clarity. The preferred values of C_{80} are between 0 and -4 dB. According to Beranek's analysis of several concert halls, highly successful ones have a C_{80} between -2.7 and -3.7 dB. Their expressions can be found in Eq. 1 and Eq. 2.

$$C_{50} = 10 \log \left(\frac{\int_{0ms}^{50ms} h^2(t) dt}{\int_{50ms}^{\infty} h^2(t) dt} \right) \quad (1)$$

$$C_{80} = 10 \log \left(\frac{\int_{0ms}^{80ms} h^2(t) dt}{\int_{80ms}^{\infty} h^2(t) dt} \right) \quad (2)$$

where $h(t)$ is the impulse response.

Clarity and reverberance are inversely correlated, so rooms with high reverberation suffer from a loss of clarity, and rooms with low reverberation times enjoy a richness of clarity. A measure of each

is usually desired. Achieving clarity demands maximizing the direct sound and the very early sound reflections that arrive just after the direct sound [18].

3.3 Speech Transmission Index (STI)

Speech Transmission Index is a magnitude related to the speech intelligibility in a room. It is obtained through the determination of the modulation transfer function (*MTF*), and it is calculated for octave bands from 125 Hz to 8 kHz. The STI descriptor takes into account band-pass limiting, noise, reverberation, echoes and nonlinear distortion. Then, returns a value from 0 to 1 whose subjective meaning can be interpreted from Table 1. More details and specifications of this descriptor can be found in the standard IEC 60268-16 [19].

Table 1: STI values graded on a subjective scale.

Intelligibility	STI value
Poor	0 to 0.3
Satisfactory	0.3 to 0.45
Good	0.45 to 0.6
Very Good	0.6 to 0.75
Excellent	0.75 to 1

3.4 Articulation Loss of Consonants (AlCons)

Like the STI, the AlCons is also a parameter related to speech intelligibility. This descriptor is an objective measurement of the loss of the sounds of the consonants, and it is obtained according equation 3 [20].

$$Al_{Cons} = 200 \cdot \frac{T_{60}^2 \cdot r^2}{V} + \alpha \quad (3)$$

Where T_{60} is the calculated reverberation time of the room, V is the volume of the room, r is the distance between the listener and the sound source, and α is a correction factor. This parameter is also tied to a subjective scale as shown in Table 2.

Table 2: AlCons values graded on a subjective scale.

Intelligibility	STI value
Ideal	$\leq 3\%$
Very good	3 to 8%
Good	8 to 11%
Poor	11 to 20%
Worthless	$\geq 20\%$

3.5 Sound Strength (G)

The magnitude of the sound, G, can be measured using a calibrated omnidirectional sound source as the logarithmic ratio of the sound energy (squared and integrated sound pressure) of the measured impulsive response compared to the measured response in a free field at a distance of 10 m from the sound. Its mathematical expressions, according to ISO-3382 [1], are shown in Equation 4.

$$G [\text{dB}] = 10 \cdot \log \left(\frac{\int_0^{\infty} p^2(t) dt}{\int_0^{\infty} p_{10}^2(t) dt} \right) \quad (4)$$

In the above equations, $p_{(t)}$ represents the instantaneous sound pressure of the impulsive response measured at the measurement point, while $p_{10}(t)$ denotes the instantaneous sound pressure of the impulsive response at a distance of 10 m in a free field. In such equations, $t=0$ corresponds to the onset of direct sound, and ∞ should correspond to a time that is greater than or equal to the point at which the decay curve has decreased by 30 dB. Typical values, according to the International Standard [1], range from -2 to +10 dB.

3.6 Lateral Fraction (LF)

The lateral fraction is an indicator introduced by Barron and Marshall [21] and it quantifies the amount of lateral sound energy that arrives at a seat in a hall. This parameter can be obtained measuring the arriving energy using a figure-8 microphone and an omnidirectional one, with an integration time of 5-80 ms and 0-80 ms respectively. Then, following equation 5, LF_{Early} can be obtained.

$$LF_{Early} = \frac{\int_{5ms}^{80ms} p_8^2(t) dt}{\int_{0ms}^{80ms} p^2(t) dt} \quad (5)$$

where $p_8(t)$ is the pressure measured by the figure-8 microphone with its null axis pointed towards the source and $p(t)$ is the pressure measured by an omnidirectional microphone at that same point. The bidirectional microphone picks up only the lateral sound waves while the other transducer captures all the acoustic energy that gets to the measurement point.

In a similar way, the LF_{Late} parameter can be calculated using a different integration time as shown in equation 6

$$LF_{Late} = \frac{\int_{80ms}^{\infty} p_8^2(t) dt}{\int_{0ms}^{\infty} p^2(t) dt} \quad (6)$$

3.7 Direct to Reverberant Energy Ratio (D/R)

The direct to reverberant ratio (D/R) expresses the ratio, at a given location, of the sound pressure level of a direct sound emitted by a directional source to the sound pressure level of the reverberated sound originating from the same source. The D/R is calculated through equation 7. The distance from the source at which this parameter is 0 dB (i.e., the direct sound and reverberant sound pressure levels are equal) is called the critical distance.

$$D/R [\text{dB}] = 10 \cdot \log \left(\frac{\int_0^q p^2(t) dt}{\int_0^{\infty} p^2(t) dt} \right) \quad (7)$$

where $p(t)$ is the sound pressure and q indicates the time where the direct sound ends.

3.8 Interaural Cross-Correlation and Interaural Cross-Correlation Function

In the context of binaural recordings, the spatial impression of a room can be estimated using the interaural cross-correlation coefficient (IACC). This parameter provides information about the similarity between the left and right ear signals, quantifying the spatial effect and envelopment. A value of 1 for IACC indicates that the left and right ear signals are identical, while a value of 0 indicates complete dissimilarity (no correlation). The normalized interaural cross-correlation function (IACF) is defined in Equation 8, and calculates the correlation between the left and right ear signals over a specified time interval.

$$\text{IACF}_{t_1/t_2}(\tau) = \frac{\int_{t_1}^{t_2} p_L(t) + p_R(t + \tau) dt}{\sqrt{\int_{t_1}^{t_2} p_L^2(t) dt \cdot \int_{t_1}^{t_2} p_R^2(t) dt}} \quad (8)$$

In this equation, p_L and p_R represent the impulse response of the left and right channels, respectively, in a binaural room impulse response (RIR). The integration is performed over the specified time interval $[t_1, t_2]$, and τ represents the time lag. To obtain the interaural cross-correlation coefficient (IACC), the maximum absolute value of the IACF is taken over a specific time range, typically within the range of -1 ms to +1 ms, as shown in Equation 9.

$$\text{IACC}_{t_1/t_2}(\tau) = \text{Max}|\text{IACF}_{t_1/t_2}(\tau)| \quad \text{for } -1\text{ms} < \tau < 1\text{ms} \quad (9)$$

The IACC represents the maximum correlation value within the specified time range, indicating the degree of similarity between the left and right ear signals in terms of spatial perception.

3.9 Listener Envelopment (LEV)

Several authors have proposed definitions for the Listener Auditory Envelope (LEV), such as Morimoto et al. [22], Soulodre [23], and Wakuda et al [24]. Griesinger's definition [25] summarizes other authors' definitions of LEV: "The Listener's Auditory Envelope is the impression of the sound coming from the sound source surrounding the listener, not the width of the sound source, and the amount the listener feels inside/of the envelope." Research [26] shows that this depends on several physical factors, such as the late-arriving reflective sound energy from the initial sound, the angular distribution of the late-arriving sound energy, the frequency content of the sound source, different reverberation times in different frequency bands, type of sound source, and the amount of temporal fluctuations and interaural intensity in the listener's ear. Its mathematical expression, according to Beranek [27], can be seen in Equation 10.

$$\text{LEV} [\text{dB}] = 0.5 G_{late,mid} + 10 \log L F_{late,mid} \quad (10)$$

Where G_{late} is the reverberant sound intensity and $L F_{late}$ is the late energy from lateral reflections. "Mid" means measurements made at mid frequencies. G_{late} can be expressed as a function of intensity G and clarity C_{80} , as shown in Equation 11.

$$G_{late} = G - 10 \log \left(1 + \log^{-1} \frac{C_{80}}{10} \right) \quad (11)$$

According to ISO 3382 [1], typical values are in the range of -14 to +1 dB. According to Beranek, LEV values in popular auditoriums can vary between -2 and 2, the latter being considered more immersive.

3.10 Autocorrelation Function and τ_e

The Autocorrelation Function (ACF) is a measure of similarity between two signals, obtained by performing point-to-point multiplications and summing the results. When the signals are identical, the sum will be a large positive number, indicating high similarity. Conversely, if the signals are random, the sum will involve positive and negative contributions, resulting in a smaller value, indicating dissimilarity [28]. The autocorrelation function is defined by Equation 12.

$$\Phi_p(\tau) = \lim_{T \rightarrow \infty} \frac{1}{2T} \int_{-T}^{+T} p'(t) \cdot p'(t + \tau) dt \quad (12)$$

Where $p'(t) = p(t) \cdot s(t)$, and $s(t)$ represents the sensitivity of the ear (often approximated as the A-weighted impulse response) for practical purposes. When plotting the similarity between the waveform and its time-shifted version as a function of the time-shift, the resulting curve, known as the running autocorrelation function (r-ACF), exhibits a larger positive maximum at zero time-shift (when the signals are identical), and smaller values for larger time shifts.

The parameter τ_e denotes the effective duration of the r-ACF, defined as the time delay at which the r-ACF envelope reaches -10 dB. This value can be obtained by extrapolating the initial decay rate of the energy decay curve to -10 dB. It also can be approximated by the median value, τ_e mid, derived from the 95% percentile [28]. A graphical representation of this procedure can be seen in Figure 2.

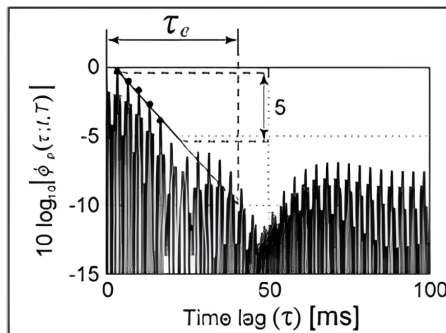


Figure 2: Determination of the effective duration extracted from the running ACF [28].

3.11 Centre Time (TS)

The centre time (TS) is the time of the centre of gravity of the squared impulse response [1]. It is measured in seconds and it is calculated by using Equation 13.

$$T_S = \frac{\int_0^\infty t \cdot p^2(t) dt}{\int_0^\infty p^2(t) dt} \quad (13)$$

TS avoids the discrete division of the impulse response into early and late periods. This parameter, together with C parameters, relates to perceived definition, clarity, or the balance between clarity and reverberance, as well as to speech intelligibility.

3.12 Stage Parameters

The stage parameters were introduced in 1989 by A. C. Gade [29] and are incorporated in ISO 3382 [1]. They are classified into ST_{early} and ST_{late} , and their calculations are represented in Equations 14 and 15, respectively.

$$ST_{early} = 10 \log \left(\frac{\int_0^{0.02} p^2(t) dt}{\int_0^{0.01} p^2(t) dt} \right) \quad (14)$$

$$ST_{late} = 10 \log \left(\frac{\int_0^1 p^2(t) dt}{\int_0^{0.02} p^2(t) dt} \right) \quad (15)$$

Where p represents the sound pressure of the impulsive response as a function of time. Early support relates to ensemble cohesion, i.e. the ease with which musicians can hear each other within an orchestra. However, direct sound influences, delay time and reflections from nearby surfaces are not considered. Late support refers to the perceived reverberance, i.e. the acoustic response of the room as perceived by the performer.

According to Gade's recommendations, the optimal ST_{early} values for a concert hall are around -14.6 dB, while for chamber music halls they are -9 dB. On the other hand, according to Bistafa [30], a value of -9.5 dB is recommended for public speaking rooms.

For typical ST_{late} values, a range mentioned by Beranek goes from -12 to -15 dB [14].

3.13 Echo Speech and Echo Music

Echo Speech and Echo Music are two descriptors formulated by Dietsch and Kraak in 1986 [31] in order to determine whether a reflection or set of reflections are perceived as an echo. The echo criterion is given by equation 16

$$EK(\tau) = \frac{t_s(\tau) - t_s(\tau - \Delta\tau_E)}{\Delta\tau_E} \quad (16)$$

where $\Delta\tau_E$ is the critical time interval over which the ratio of increase of energy is analysed (9 ms for speech and 14 ms for music), and t_s is a modified version of the center time formula, as it appears in equation 17

$$t_s = \frac{\int_{t=0}^{\tau} t |p(t)|^n dt}{\int_{t=0}^{\tau} |p(t)|^n dt} \quad (17)$$

where $p(t)$ is the amplitude of the sound pressure over time and the exponent n is given by the values found in Table 3, which also includes the echo criterion thresholds for speech and music beyond which the reflections are perceived as a disturbing echo. There are two values for each motif, where the lower (stricter) ones (EK [10%]) apply for people with trained hearing.

Table 3: Echo threshold according Dietsch and Kraak's criterion.

	Bandwidth of test signal [Hz]	n	$\Delta\tau_E$ [ms]	EK [10%]	EK [50%]
Speech	700-1400	2/3	9	0.9	1.0
Music	700-2800	1	14	1.5	1.8

3.14 Preferred values of acoustical parameters

The adequacy of the acoustic parameters in an auditorium is essential to ensure sound quality in both musical events and speeches. These parameters not only influence the perception of the audience, but also the experience of the performer or speaker.

Table 4 presents the acoustic parameters considered ideal for an auditorium. These data are the result of comparisons and preference surveys conducted in various halls around the world. Such magnitudes provide a reference to determine the quality of the acoustic parameters measured in relation to the intended use of the hall.

Table 4: Recommended values for several parameters for the concert hall and speech [32, 33, 34, 35, 36].

Parameters (mid-frequency)	Auditorium	
	Speech	Concert Halls
Reverberation time (RT)	$1.18 \leq RT \leq 1.7$ s	$1.8 \leq RT \leq 2.2$ s
Early decay time (EDT)	$0.3 \leq EDT \leq 0.8$ s	$1.8 \leq EDT \leq 2.2$ s
Clarity	$+1 \text{ dB} \leq C_{50}$	$-2 \leq C_{80} \leq +2$ dB
IACC	-	0.5
Sound Strength (G)	10 dB	0.7 dB
Lateral energy fraction (LF)	-	$0.1 \leq LF \leq 0.35$

4. Procedure

4.1 Auditorium Description

The “Auditorio de la Paz”, built in 2006 under the direction of the renowned architect Clorindo Testa at the request of the international Buddhist community “Soka Gakkai”, represents an emblematic space destined mainly for cultural and religious activities. The exterior of the building is shown in Figure 3.



(a) View from the outside.



(b) View from inside the building to the outside.

Figure 3: Exterior view of the building.

Located on a $4,450 m^2$ lot on the corner of Donado and Mendoza Streets in the neighborhood of Villa Urquiza, in the Autonomous City of Buenos Aires, Argentina [37], this imposing building occupies a prominent place in the urban fabric. The location of the site can be seen in Figure 4.



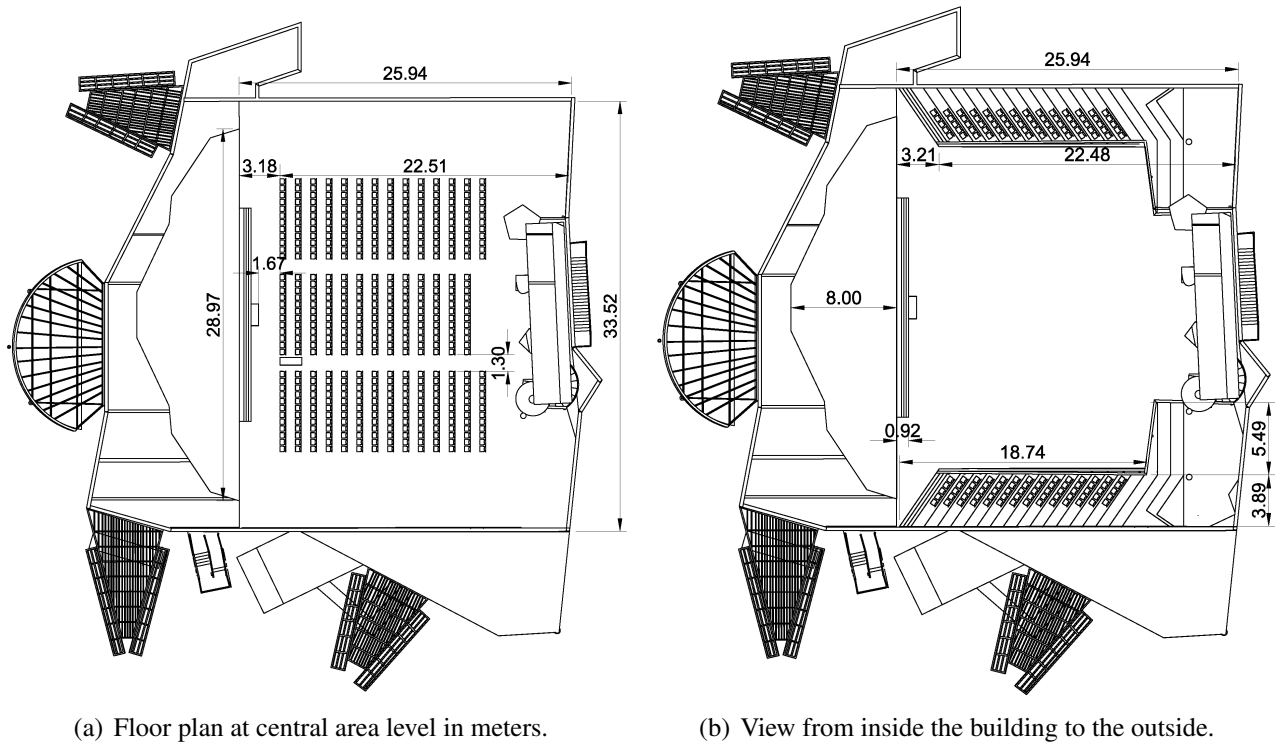
Figure 4: Location of the Auditorium of “La Paz Soka Gakkai”.

Initially conceived as a group of reformist Japanese educators inspired by the philosophy of Nichiren Buddhism, the Soka Gakkai has evolved under the leadership of such figures as Tsunesaburo Makiguchi [38], Josei Toda [39] and Daisaku Ikeda [40] to encompass a wide range of activities dedicated to peace, culture and education around the world [41].

Access to the building, which consists of three floors, including a subway level that houses parking, storage, the machine room and music rehearsals, is via the interior plaza, up a curved podium with two wide steps, partially covered by a large glass canopy with a metal frame. Once inside, visitors are greeted by a large foyer leading to the various rooms on the second floor, as well as the stepped ramps leading to the Auditorium, located in the center of the architectural ensemble.

The Auditorium, strategically located on the second floor, emerges as the primary epicenter of the entire architectural ensemble. Its access, delineated by two staggered ramps that unfold from the main hall, provides a fluid and elegant experience, turning the journey to the auditorium into a serene stroll.

With a total capacity of 950 seats, the seating arrangement in the central area is presented as a focal point, divided into three zones, each housing 156 seats, while on the sides are elevated boxes, each with 75 seats. This versatile design of the auditorium allows it to adapt to a wide range of activities, from religious events to cultural manifestations, facilitating the removal of seats or modifying the layout of the stage according to the needs of the moment. In the event that the space is not used as a religious venue, sliding doors discreetly conceal the altar, meticulously imported from Japan. [42]. Figure 5 shows the top view of the floor plan at central area level and the stalls.



(a) Floor plan at central area level in meters.

(b) View from inside the building to the outside.

Figure 5: Floor plan of the stalls in meters.

The interior of the auditorium can be seen in Figure 6.

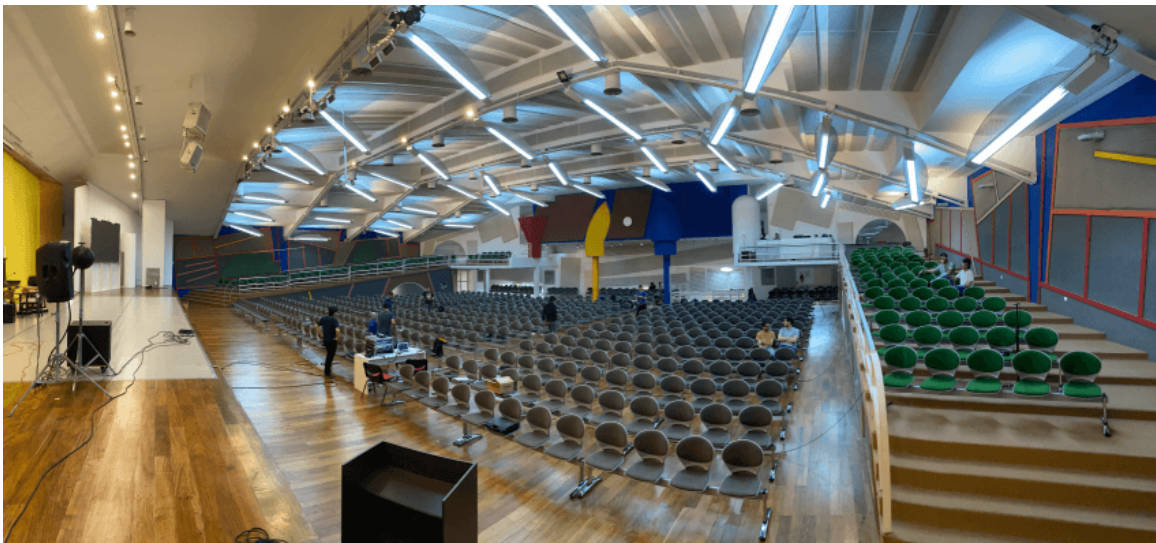


Figure 6: View of the interior of the auditorium.

Inside the auditorium hall, various elements have been arranged that contribute significantly to the acoustic quality of the space. The walls have been lined with carpeting, as well as those adorned with wooden slats, contribute to the absorption and diffusion of sound in a balanced manner. It is relevant to note that these panels are mainly concentrated on the side walls of the auditorium, although their distribution is not uniform on both sides. On the right side of the auditorium, some windows have been covered with absorption panels. This offers different acoustical features from glass windows. On the other hand, at the back of the auditorium, wooden slats have been installed with the function of acting as acoustic diffusers, ensuring a homogeneous dispersion of sound throughout the space. This can be seen in Figure 7



Figure 7: Room acoustic conditioning.

The ceiling, on the other hand, has been specially designed to enhance the sound quality inside the auditorium. Perforated sheet metal soffits have been strategically distributed to maximize sound reflection and absorption, thus contributing to an optimal listening experience for the audience.

As for the auditorium floor, it has been covered with a thick, high traffic carpet. This choice is not only for aesthetic purposes, but is also oriented to add absorption to the enclosure, as well as to support the constant flow of people passing through the enclosure, offering comfort and durability at the same time.

The entrance to the auditorium, as previously mentioned, is characterized by the presence of ramps covered with rubber on the floor. This design establishes a connecting corridor between the auditorium and the building hall. This corridor not only facilitates the transit of attendees, but also plays a crucial role in optimizing the acoustic coupling between the two spaces. It is relevant to note that this zone exhibits a remarkable acoustic absorption capacity, which contributes significantly to improve the sound quality inside the enclosure. This zone is shown in Figure 8



Figure 8: Access ramp, which connects the building's hall with the auditorium.

On the first floor of the auditorium, the final rows of seats are protected by the balcony. Here, the seats are composed mainly of plastic, with two specific areas lined with lightly padded chairs, providing additional comfort to the spectators. On the other hand, in the lateral stalls, a similar seating arrangement is observed, albeit with variations in color that distinguish them from those on the first floor. Details on the appearance of the seats can be seen in Figure 9.



(a) First floor seating.

(b) Stalls seats.

Figure 9: Images of the different seats in the auditorium.

The stage has a width of 28.97 meters, a depth of 8 meters and a height of 1.5 meters. These measures provide a considerable space to accommodate a large audience and facilitate the development of various activities, from conferences to artistic presentations.

The stage floor presents a mixed composition, highlighting the use of a floating floor covering at its ends. In contrast, the central area is covered with a linoleum floor, a material known for its durability and ease of maintenance, suitable for withstanding the constant traffic of people.

On the other hand, the auditorium's ceiling consists of a smooth concrete surface, which has been

painted to provide a uniform and aesthetically pleasing appearance. This finish contributes to sound reflection and absorption, which can be beneficial to the acoustic quality of the space, especially during events requiring good sound intelligibility.

At the back of the enclosure there are movable plaster panels, which can fulfill both aesthetic and functional functions. These panels provide the necessary flexibility to modify the layout of the space according to the specific needs of the event or activity to be held. Figure 10 shows the photo of the stage. It is worth mentioning that, at its ends, it has openings to allow circulation towards the back of the stage.

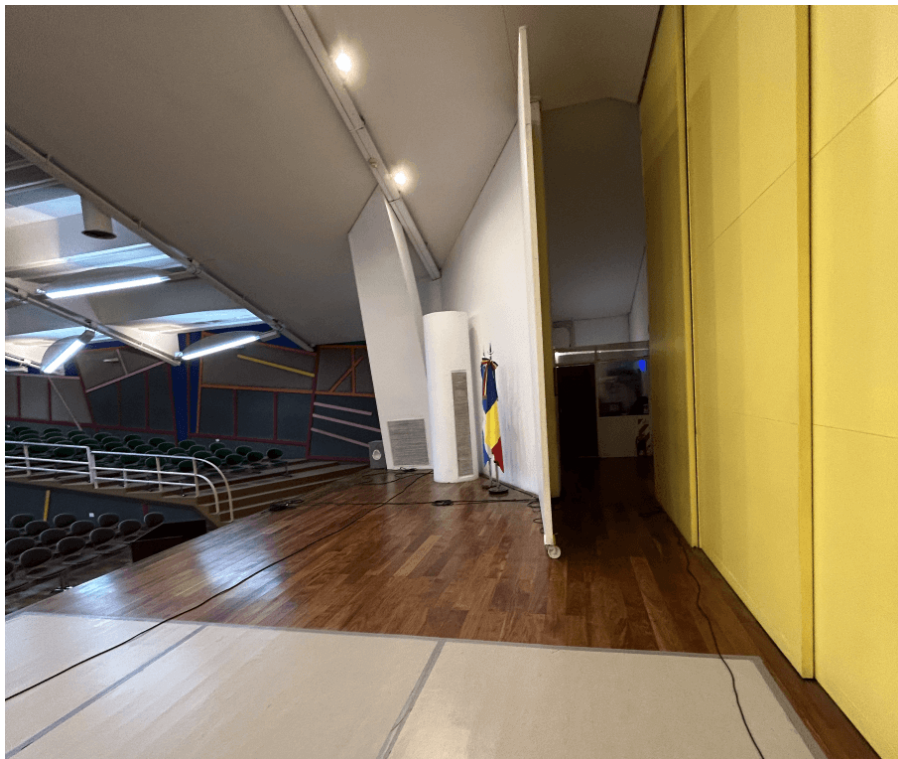


Figure 10: Stage picture.

Despite the absence of specific information on the acoustic properties of the materials used inside the auditorium, a table, presented as Table 5, has been developed that compiles the absorption coefficients of similar materials [43, 14]. This resource provides a useful reference to evaluate and compare the acoustic efficiency of the different elements present in the enclosure.

Table 5: Absorption coefficients of similar materials to the ones present in the Theater[43, 14].

Material	Frequency [Hz]					
	125	250	500	1000	2000	4000
Lightly upholstered unoccupied seats	0.36	0.47	0.57	0.62	0.62	0.60
Carpet heavy, on concrete	0.02	0.06	0.14	0.37	0.60	0.65
Carpet, thin, cemented to concrete (floor)	0.02	0.04	0.08	0.2	0.35	0.4
Layer of rubber, cork, linoleum and underlay or vinyl and underlay, stuck to concrete	0.02	0.02	0.04	0.05	0.05	0.10
Microperforated absorber	0.08	0.27	0.70	0.35	0.11	0.04
Smooth concrete, painted or glazed	0.01	0.01	0.01	0.02	0.02	0.02
Linoleum or vinyl stuck to concrete	0.02	0.02	0.03	0.04	0.04	0.05

According to the descriptions provided in Beranek and Cox's book, it is established that the seats located in the stalls are lightly upholstered with carpet.

4.2 Measurement

In conducting measurements in the auditorium in question, various specialized materials and equipment were used, among which the following stand out: 15 Earthworks M50 omnidirectional microphones, 1 Soundfield SPS200 Ambisonic microphone, 1 Kemar binaural artificial head, 1 RME Octamix preamplifier, 1 RME UFX+ audio interface, 1 Outline GSR omnidirectional loudspeaker along with its 118 subwoofer, 1 JBL EON 515 XT loudspeaker, 1 Svantek SVAN979 sound level meter and 1 Svantek SV36 sound level meter calibrator.

The measurement process begins with planning to optimize the limited time available in the auditorium. For this purpose, a sketch is prepared reflecting the possible positions of the microphones, taking into account both the floor plan of the enclosure and the symmetry of its dimensions. Given the similarity between the surfaces and dimensions of both sides of the auditorium, it was decided to place the microphones only on the left side, extrapolating the results to the right side. Except for the Soundfield microphone, which was moved to various areas of the auditorium.

For the sound sources, three positions were established: one in the center of the stage and two on the sides. The distribution of the microphones and sound sources is shown in Figure 11 of the report.

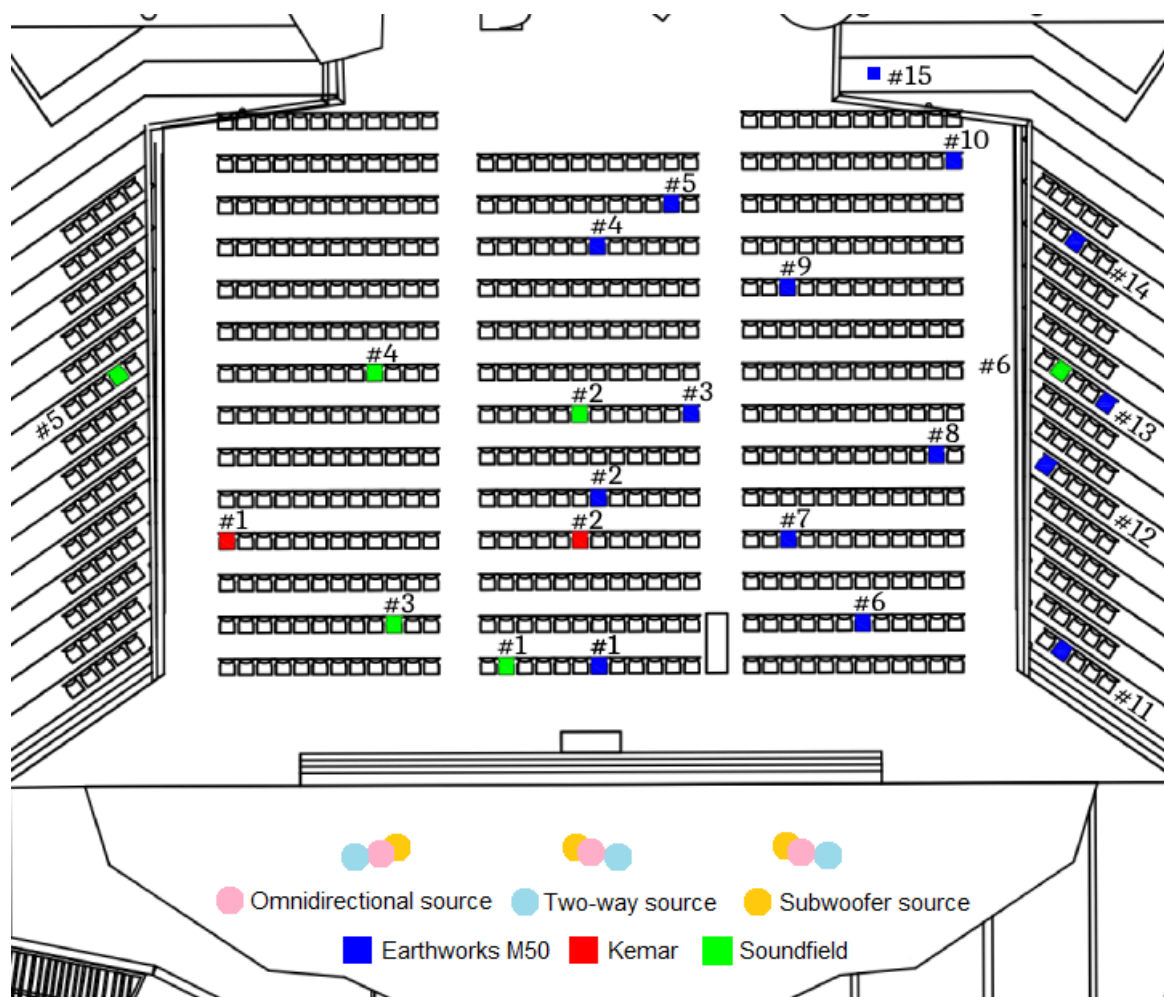


Figure 11: Microphone and sound sources positions on the auditorium for measurement.

In Figure 11 squares represent microphones and circles are sound sources. The blue squares represent the Earthworks microphone, the red ones represent the Kemar microphone, the green ones the Ambisonics microphone. On the other hand, the pink circles are the omnidirectional source, the cyan ones are the two-way source and the orange ones are the subwoofer source.

A small number of microphones are used to measure the stalls. Following the principle of symmetry observed in the stalls, four strategic measurement positions were established. In order to get the measurements to complete symmetry principle, the three sound source positions were measured: at the center of the stage and both sides. Although this approach might imply certain limitations in the completeness of the data collected, an attempt was made to maintain methodological consistency and to maximize the available information within the given circumstances. On the other hand, the sound operator is located at the end of the stalls, so it was decided to perform the measurements in that position.

In order to obtain accurate and exhaustive measurements of the acoustic parameters of the stage, a second measurement session is carried out. In this instance, a specific arrangement of the microphones is required, configured in the form of a cross and located at a distance of 1 meter from the sound source in question. Earthworks M50 microphones were used, positioned at a height of 1.6 meters. This arrangement was made so that the omnidirectional sound source was located in the center of the stage, thus ensuring an equidistant distribution of the microphones around the source. The system was also designed to improve the acoustic characteristics of the stage. This is shown in Figure 12



Figure 12: Measurement of stage parameters.

To carry out the measurement, the Earthworks microphones were calibrated using the Svan calibrator and a 1 kHz frequency signal at 94 dB SPL. Simultaneously, the sound level meters were calibrated and the background noise was measured, thus establishing an adequate reference frame for subsequent measurements.

To set up the sinusoidal logarithmic sweep, the frequency range that the dodecahedron can reproduce was considered, selecting a spectrum ranging from 20 to 16,000 Hz. The duration of this sweep was set at 40 seconds, with the objective of achieving an optimal signal-to-noise ratio.

In addition, as part of the methodology employed, three different anechoic recordings were used: one of a female lyrical character, another of a percussive drum performance and a third of a clarinet. These recordings were played through two types of sound sources in the three predefined positions: the omnidirectional source for the recording of the logarithmic sweep signal and the directional source for the anechoic recordings.

The recording process resulted in a total of 25 audio files for each source position on the auditorium floor, distributed as follows: 20 corresponding to the Earthworks microphones, 2 to the Ambisonics microphones and 3 to the Kemar microphones. For the balcony and under-balcony areas, a total of 14 audio files were obtained for each source position.

To obtain the Reverberation Impulse Responses (RIRs) of the sinusoidal sweep generation, a convolution procedure is carried out with the inverse filter, using Farina's Aurora plugin. Subsequently, using the same software, these RIRs are processed in order to obtain a series of relevant acoustic parameters.

The acoustic parameters derived from this process include the Early Decay Time (EDT), the Signal-to-Noise Ratio (SNR), the reverberation times T₂₀ and T₃₀, as well as the clarity parameters C₅₀ and C₈₀. In addition, the acoustic intelligibility parameters, such as Ts, STI, ST1, ST2 and IACC, are calculated using the aforementioned software.

For the determination of the parameters LF (lateral fraction) and D/R (Direct-Reverberation Ratio), the acoustic analysis tool EASERA is used. On the other hand, the parameter τ is calculated by

means of a specific script (ACF) developed in the MATLAB environment.

To determine the LEV parameter, which is intrinsically related to the G and C_{80} parameters, Equation 10 is used to calculate the GLate parameter in specific frequency bands and for individual microphone positions. Subsequently, the average of the G_{Late} and LF_{Late} parameters in the 500, 1,000 and 2,000 Hz frequency bands is obtained, resulting in the LEV parameter for all microphone positions on the auditorium floor.

On the other hand, the LF (lateral fraction) parameter is determined from the recordings made with the Ambisonic microphones in the sound field. When converting from format A to format B, the W and Y channels are obtained, which represent the omnidirectional and figure-of-eight diagrams, respectively. These channels provide crucial information for calculating the LF parameter, which contributes to a more complete understanding of the spatial distribution of sound in the auditorium.

5. Results and Discussion

5.1 Background Noise

In order to assure a sufficient signal to noise ratio, background noise level was registered before proceeding with the room impulse response measurements. Results are shown in Figure 13 presented per third octave bands from 125 Hz to 8 kHz without any weighted curve applied.

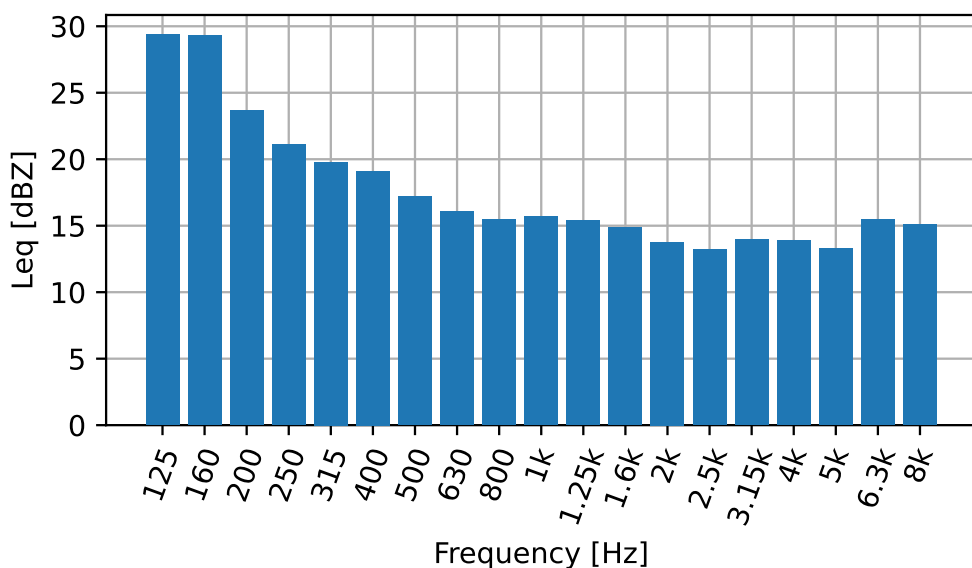


Figure 13: Background noise.

The increase of background noise in low frequencies is appreciated, but overall every third band is under 30 dB. According to Standard ISO 3382 [1], a SNR of 45 dB is required for T30 measurements. This indicates that the microphone farthest to the source should register at least 75 dBZ in lower frequencies, and around 60 dBZ in the rest of the spectrum.

5.2 EDT, T20 and T30

Measurements of reverberation time were performed and averaged across 14 microphone positions. Figure 14 shows EDT, T20 and T30 results obtained per third octave bands with the associated expanded standard deviation.

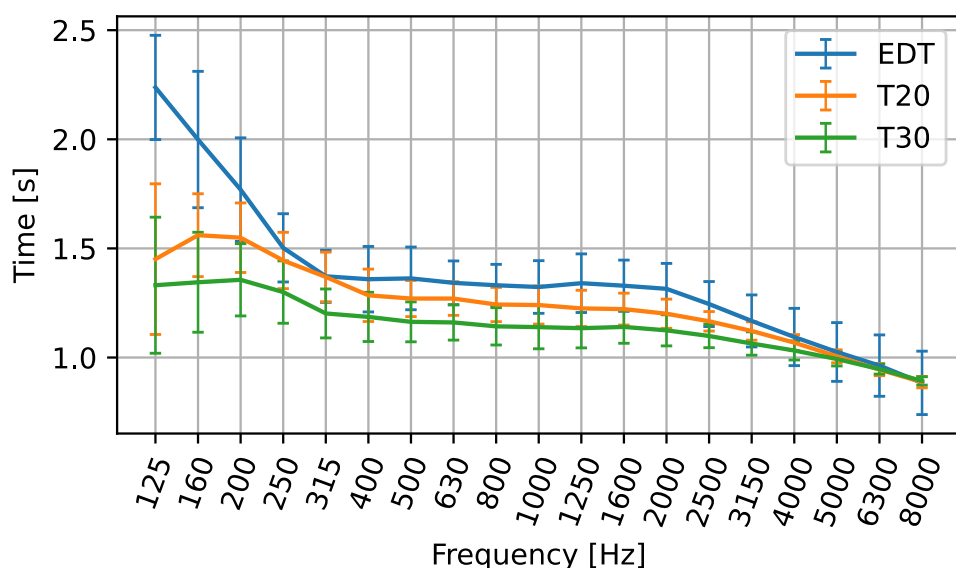


Figure 14: Reverberation time.

In general, the results show a balance between T20 and T30, since both present a similar curve over the whole spectrum.

In the lower frequency range, the reverberation time tends to be higher, as expected, since the photographs do not show any absorbing elements specifically designed for low frequencies, such as resonators. Conversely, at higher frequencies, the reverberation time decreases. This result is also to be expected, as high-frequency energy is easily absorbed by materials such as absorbent panels in the ceiling, carpeting on the walls, etc. It may even be due to the air.

Analyzing the parameters in Figure 14 with the expected values in Table 4, it can be seen that the hall presents acoustic characteristics that do not fully conform to the recommended parameters for both speech and concert halls. Regarding reverberation time (RT), at low frequencies, the values exceed the upper limit recommended for speeches (1.7 s), while at medium and high frequencies, the reverberation times (T20 and T30) are around 1.0 - 1.2 s, below the optimal range for speeches. For concert halls, RT values are significantly below the recommended range (1.8 - 2.2 s), indicating insufficient reverberation time. Concerning the early decay time (EDT), the values observed in the graph for mid and high frequencies (0.9 - 1.1 s) exceed the acceptable range for speech (0.3 - 0.8 s) and are well below the optimal range for concerts (1.8 - 2.2 s), suggesting inadequate control of early reflections for both speech and music. Therefore, the room is not fully optimized for either of these specific applications, being in an intermediate position for both speech and concerts.

It is observed that at medium frequencies, between approximately 250 Hz and 2.5 kHz, the reverberation time presents a flat curve around 1.3 s, 1.25 s and 1.2 s for each parameter, respectively. The arguably small deviation observed may indicate a uniform distribution of reverberation time in the room.

For this reason, Figure 15 shows the spacial TR across the seating area. This colormap was obtained interpolating the measurements of the 14 microphone positions.

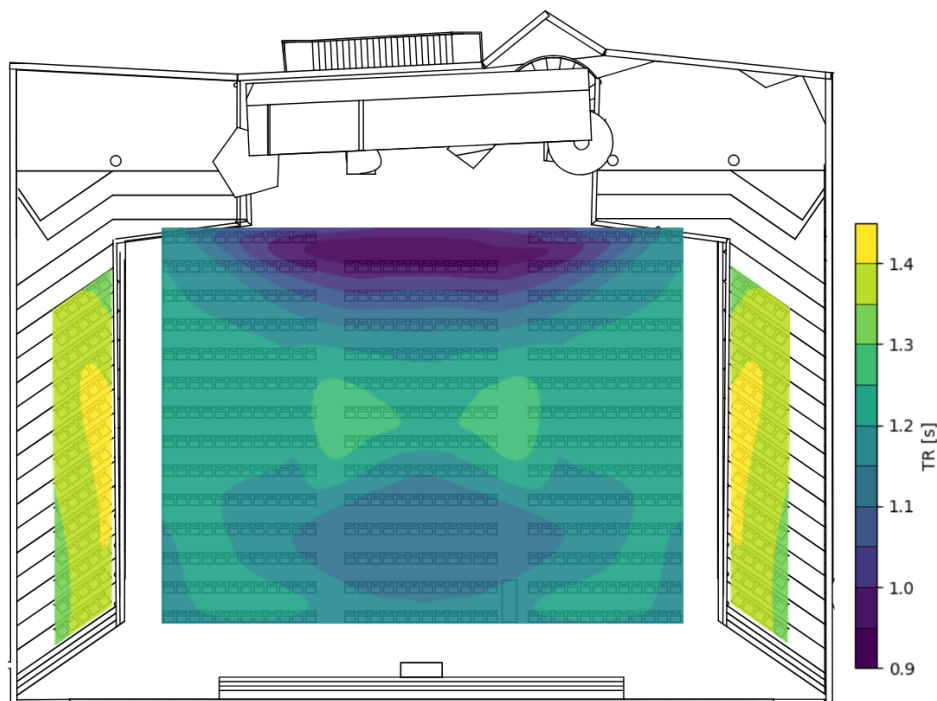


Figure 15: Spatial distribution of reverberation time (T_{20}).

Only the last seating row of the center block presents a reverberation time under 1.0 s, while the majority of the seating area shows around 1.2 s. The highest values registered can be found in the lateral blocks, reaching up to 1.4 s.

It can be seen that the Early Decay Time (EDT) values are relatively homogeneously distributed above 250 Hz, with a difference of approximately 0.7 seconds between the maximum and minimum values recorded. However, a significant increase in EDT is observed below 250 Hz.

These discrepancies, especially noticeable at the lower frequencies, suggest a lack of uniformity in reverberation control throughout the listening area. This variation could be attributed to the lack of diffusers designed to specifically address the low frequencies in the room.

The absence of low-frequency diffusers can result in uneven sound distribution in the space, affecting the acoustical perception of the audience and compromising the sound quality of the environment. Therefore, the consideration and implementation of appropriate acoustic solutions, such as the incorporation of low-frequency diffusers, could contribute significantly to improving the uniformity of reverberation control in the auditorium.

Figure 16 shows the EDT, TR_{20} and TR_{30} parameters for each microphone position. Where the darker shade of the curves correspond to the position closer to the stage.

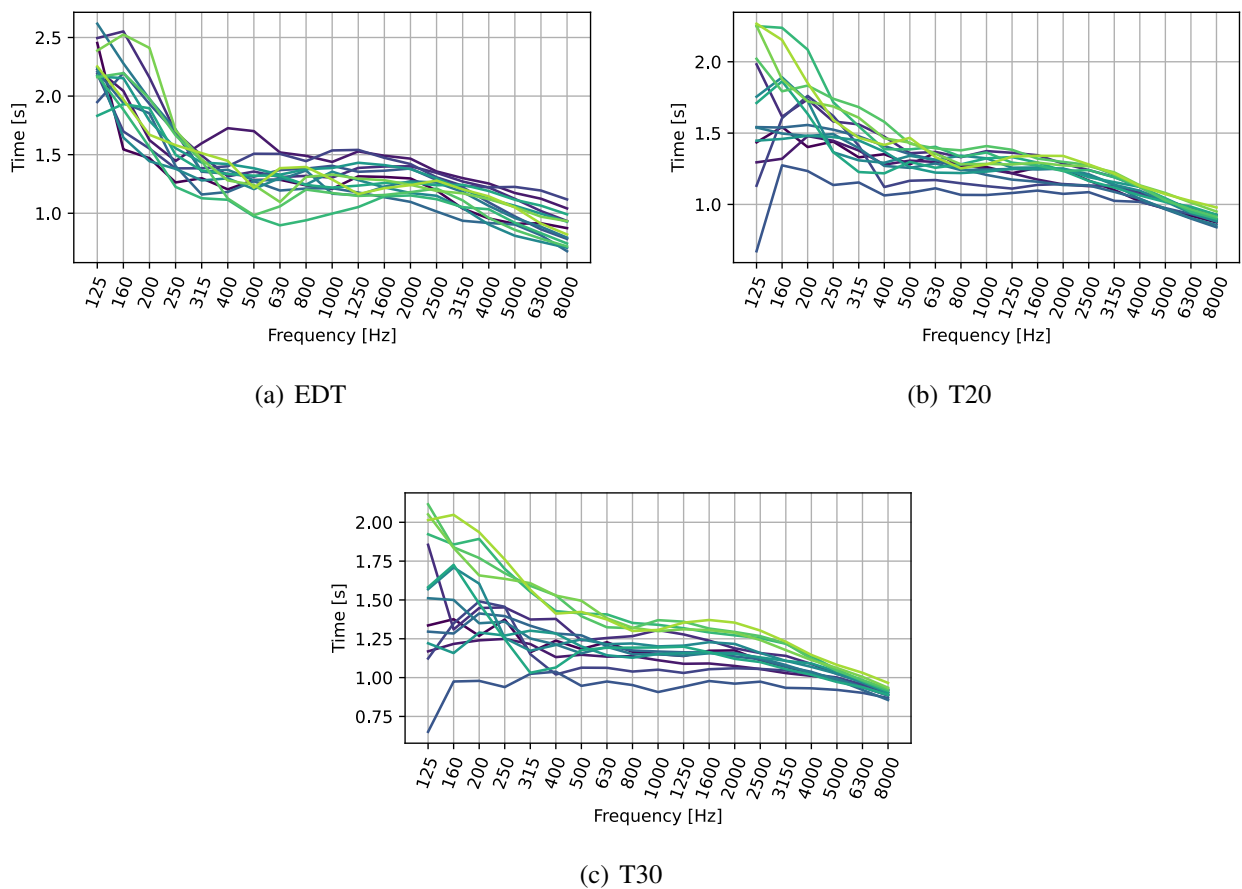


Figure 16: EDT, T20 and T30 registered across 14 microphone positions.

In the Figure of T20 and T30, it is observed that the last positions with respect to the source present a curve of higher reverberation time, while the closest ones show a lower reverberation time. In addition, the farthest microphones positions show a peak at 160 Hz, which can be attributed to reflections on the walls of the stalls.

Figure 17 shows the TR which was obtained from the subjective RIRs for 10, 100 and 350 ms.

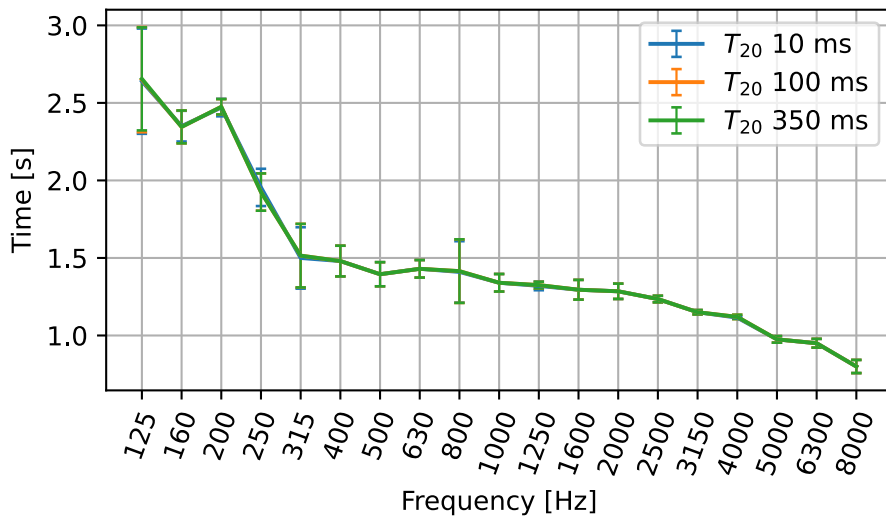


Figure 17: T_{20} values with different integration times.

The analysis of the subjective reverberation times (T20), shown in Figure 17, reveals a clear trend in the acoustic response of the room as a function of frequency. At low frequencies, from 125 Hz to 500 Hz, reverberation times are longer, reaching values close to 3.0 seconds, suggesting higher reverberation and lower sound absorption in these frequency bands. This behavior is characteristic of spaces with surfaces that effectively reflect low frequencies. As the frequency increases, between 500 Hz and 2000 Hz, a gradual and noticeable decrease in reverberation times is observed, indicating better sound absorption or dispersion at these frequencies, due to the presence of absorption in the walls of the room. At frequencies above 2000 Hz, reverberation times stabilize at around 1.0 to 1.5 seconds, indicating effective absorption of high frequencies, reducing reverberation to more controlled levels. All three data sets, corresponding to 10 ms, 100 ms and 350 ms windows, show consistency in this general trend, although the 350 ms measurements provide a more detailed and complete representation of acoustic behavior across the entire frequency range. This analysis suggests that the room under study has a variable sound absorption capacity that improves with increasing frequency.

Figure 18 shows the early decay time (EDT) obtained from the subjective RIRs for 10, 100 and 350 ms.

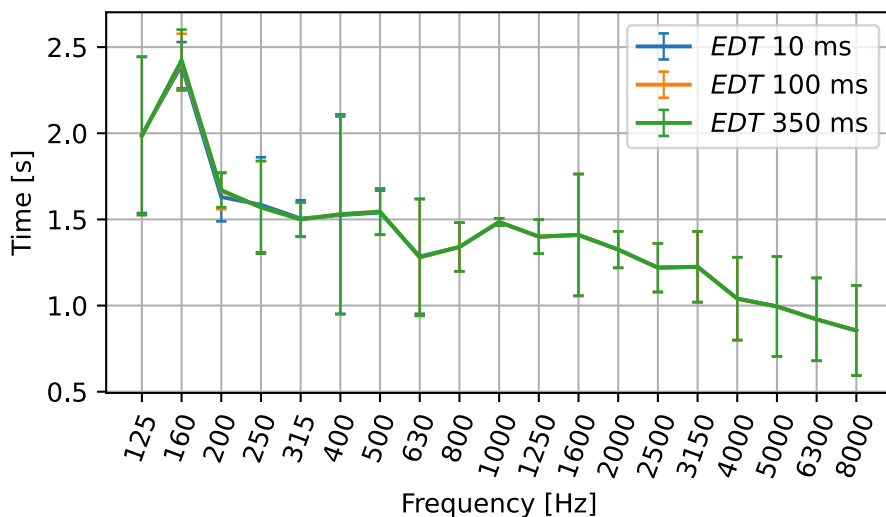


Figure 18: *EDT* values with different integration times.

The analysis of the subjective early decay times (EDT), represented in the graph provided, reveals detailed information about the behavior of the first reflections in the room as a function of frequency. At low frequencies, ranging from 125 Hz to 500 Hz, EDT values are relatively high, reaching approximately 2.5 seconds. This suggests that the first reflections at these frequencies are more persistent, which may contribute to a greater sense of reverberation and less clarity of sound in the low range. As frequencies increase, between 500 Hz and 2000 Hz, EDT values gradually decrease, indicating that the first reflections are absorbed. This pattern suggests an improvement in sound clarity and definition in the mid-frequencies, this is due to the presence of acoustic materials that efficiently absorb these frequencies. At frequencies above 2000 Hz, EDT values tend to stabilize around 1.0 to 1.5 seconds. This reflects effective absorption of high frequencies, reducing the persistence of early reflections and contributing to a more controlled and defined listening environment.

5.3 C50 and C80 (Clarity)

Figure 19 shows the results for the spatially-averaged C50 and C80 parameters, with their associated expanded uncertainty. Figures 20 and 21 show the spatial distribution of the same parameters for the 1 kHz band.

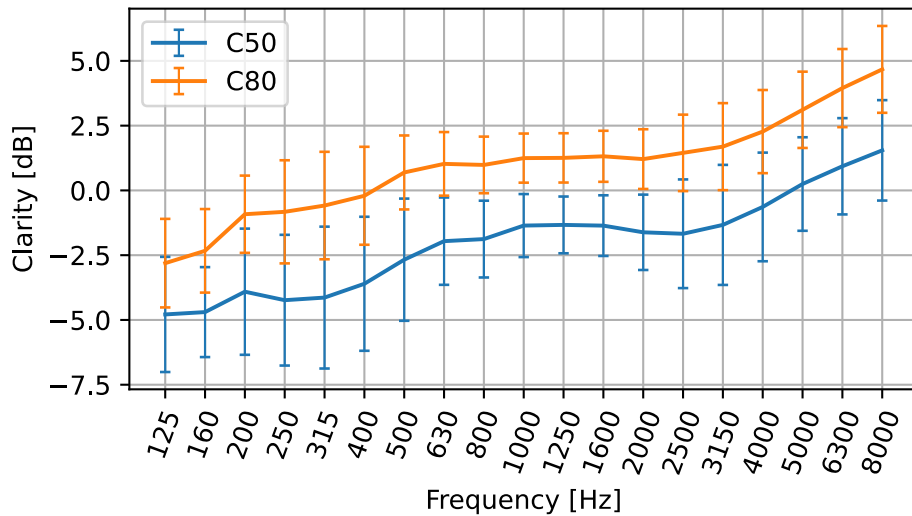


Figure 19: Spatial average of C50 and C80 measurements.

Overall, both parameters follow a similar tendency, with C80 values being approximately 3 dB higher than C50 values in the frequency range of interest. A good C50 value should be greater than 0 dB for a good speech intelligibility, but this value is only reached in frequencies higher than 5 kHz. This means that this auditorium may be slightly under-performing when used for speech purposes. Regarding the C80 values registered, it depends on the musical genre, but in general values greater than -3 dB and up to 6 dB are allowed for the majority of musical performances [44]. Thus, clarity parameters show that this auditorium is more suitable for music rather than speech applications.

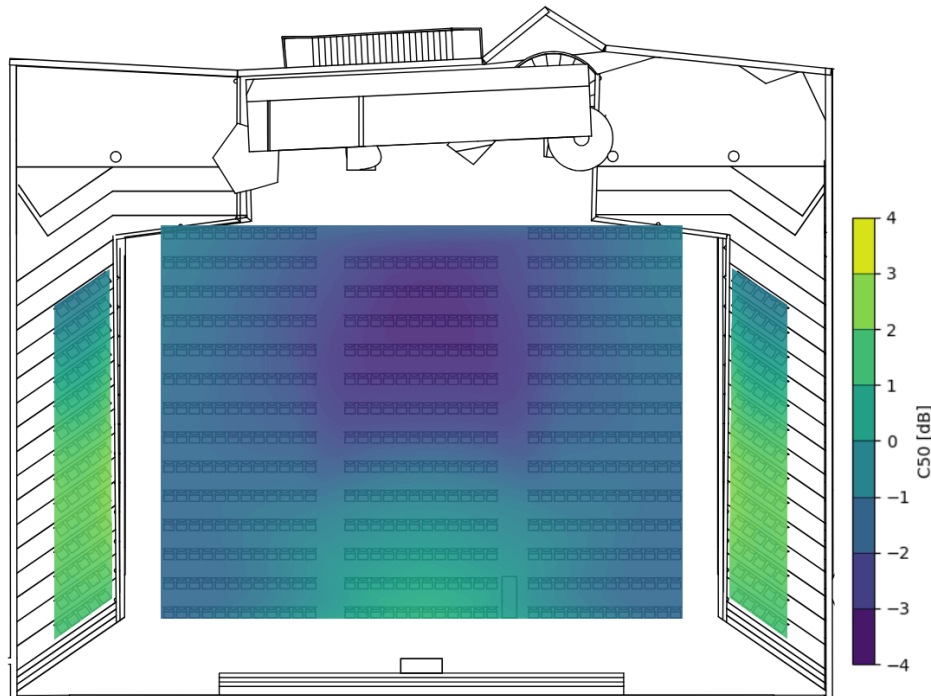


Figure 20: C50 spatial distribution for 1 kHz.

More information about the clarity parameters can be extracted looking at Figure 20. The back rows of the center block show the lowest C50 values, reaching around -3 dB. Meanwhile, the front center rows and the lateral seating area appear to be the best seats regarding speech clarity.

Regarding the C80 colormap shown in Figure 21, the scale of values is the same as the C50 image, allowing a better comparison between both figures. Same as Figure 19, a 3 dB increase from C50 to C80 can be perceived also in the spatial representation of these parameters.

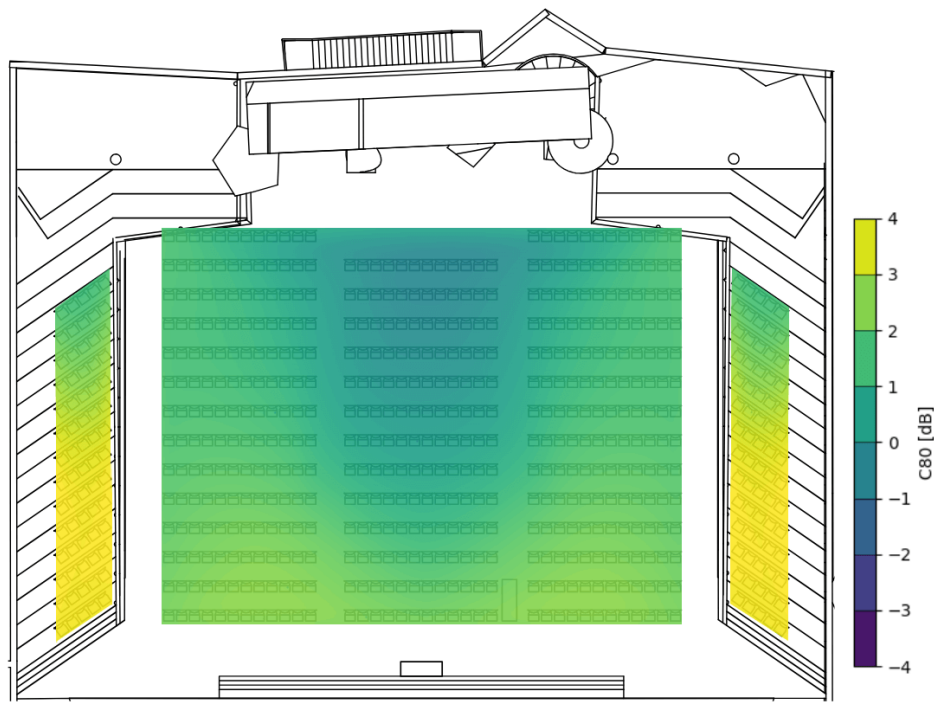


Figure 21: C80 spatial distribution for 1 kHz.

In this case, every seat presents an adequate C80 value for general musical purposes. The spatial distribution is the same as the C50 colormap.

Figure 22 shows the clarity (C_{50}) obtained from the subjective RIRs for 10, 100 and 350 ms.

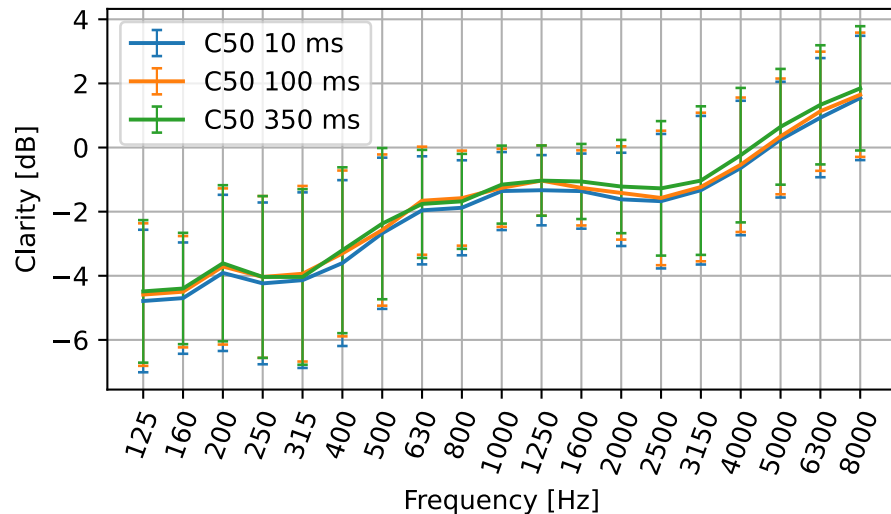


Figure 22: C_{50} values with different integration times.

Figure 23 shows the clarity (C_{80}) obtained from the subjective RIRs for 10, 100 and 350 ms.

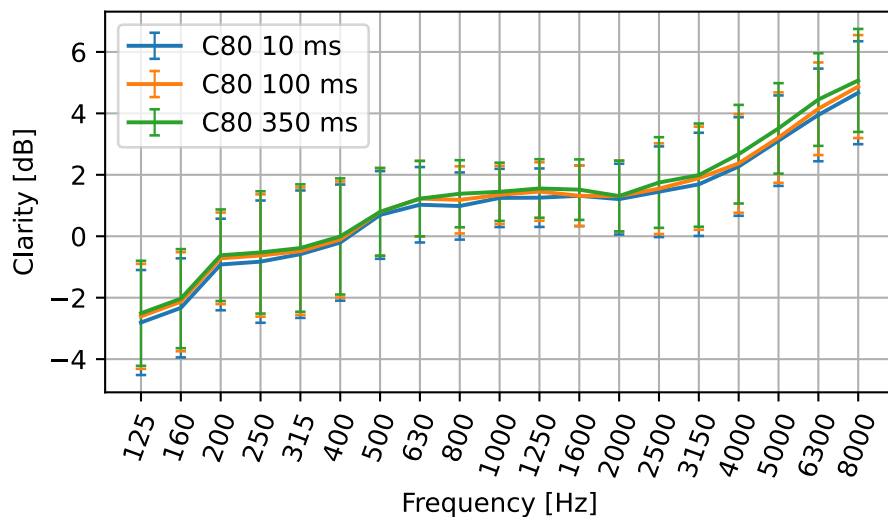


Figure 23: C_{80} values with different integration times.

It can be seen that the C_{50} and C_{80} remain with similar values for different integration windows. The 350 ms window shows a slightly higher curve, but does not differ by more than 0.5 dB with respect to the other integration intervals.

5.4 AlCons [%] and STI

The spatial average value of the AlCons parameter is $10.0 \pm 3.6 \%$. This value indicates a good intelligibility, according to Table 2, although the associated uncertainty may indicate some seating areas presenting better or worse results.

For this reason, Figure 24 shows the individual value registered by the 10 microphones positioned in the main seating area, and Figure 25 shows the spatial distribution of the AlCons parameter.

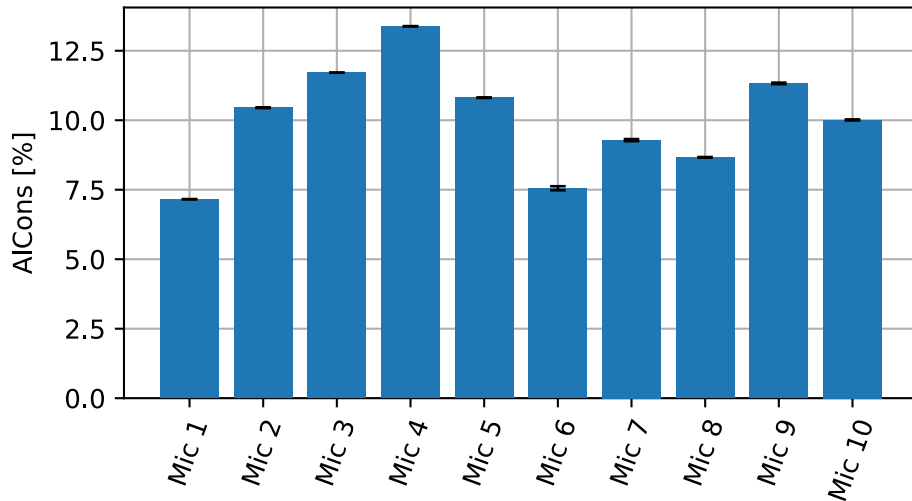


Figure 24: Obtained AlCons values for every microphone position in the main seating area.

The lowest registered value is 7.15 %, corresponding to the first microphone position located in the first row, while the maximum value is 13.4 % measured in the 11th row with the 4th microphone position.

Only the front row presents values under 8%, resulting in a very good intelligibility. On the other hand, a large seating area around the back center rows present values over 11 % (as seen in Figure 25), which indicates poor intelligibility.

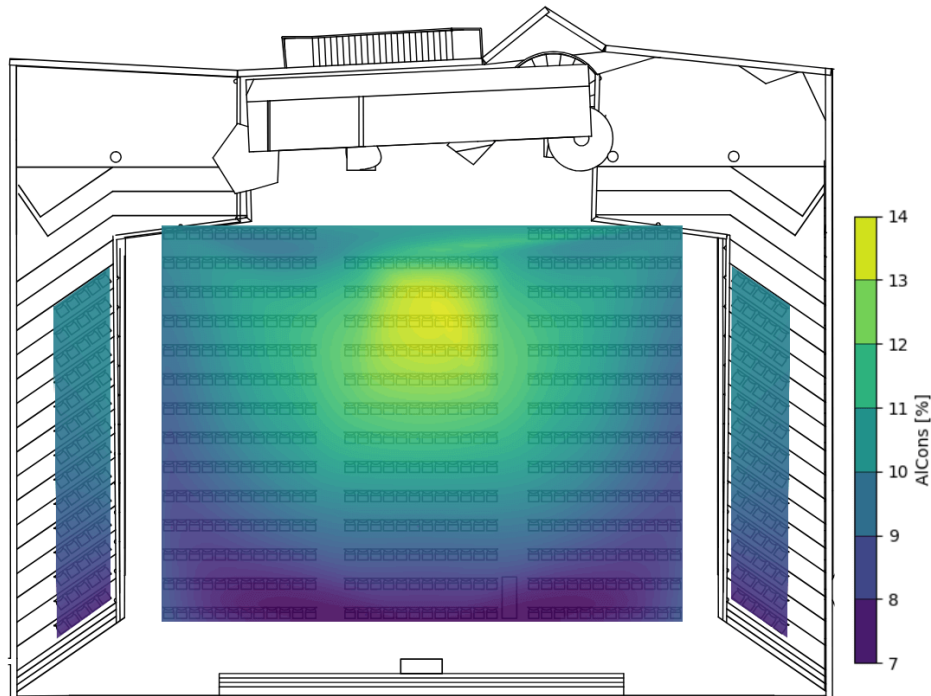


Figure 25: Spatial distribution of the AlCons parameter.

When applying the different subjective integration intervals, there were similar results along all microphone positions. For a 10 ms window, the spatial average value of AlCons is $9.8 \pm 3.5\%$. With a 100 ms window the AlCons parameter is $9.8 \pm 3.5\%$ and finally, with a 350 ms window, a value equal to $9.7 \pm 3.6\%$ is obtained. These results could indicate that the number of seats falling under the 'good intelligibility' category slightly increases when applying an integration window.

Following with the Speech Transmission Index results, Figure 26 shows a minimum value of 0.471 and a maximum of 0.587, measured at the first and 11th row, respectively. These positions correspond to the lowest and highest AlCons percentages registered. All STI values fall under the 'good intelligibility' category, which corresponds to values between 0.45 and 0.60, as seen in Figure 26.

When applying the 10, 100 and 350 ms integration window, the spatial average STI is 0.53 for every window, almost identical as the objective STI values.

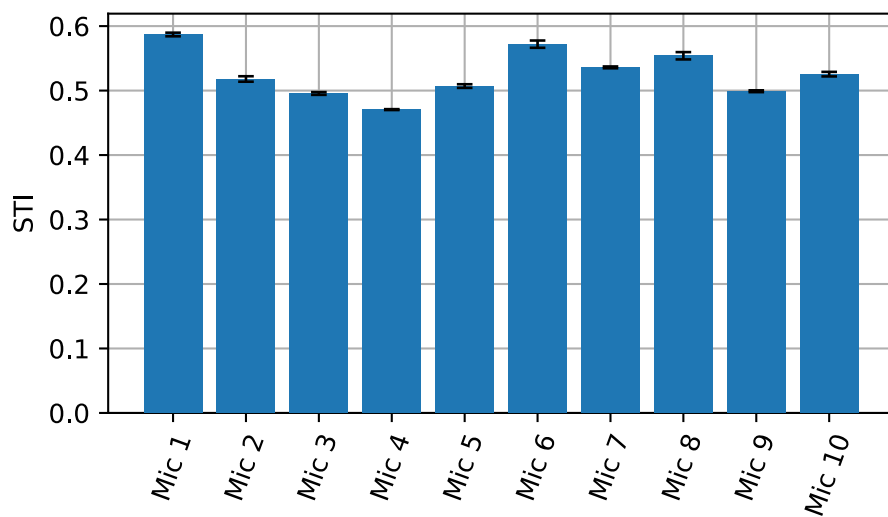


Figure 26: Individual Speech Transmission Index values registered in the main seating area.

The spatial distribution of the STI is shown in Figure 27. It can be seen that STI and AlCons colormaps are very similar but with an inverted color scale. Different from the AlCons spatial distribution shown in Figure 25, in this case the front rows do not reach the 'very good' category regarding intelligibility. Even the lowest STI values measured in the back center area still correspond to good intelligibility.

This comparison shows that AlCons values indicate three different intelligibility categories across the entire seating area, going from poor to very good, while STI values qualifies all seating positions as having good intelligibility.

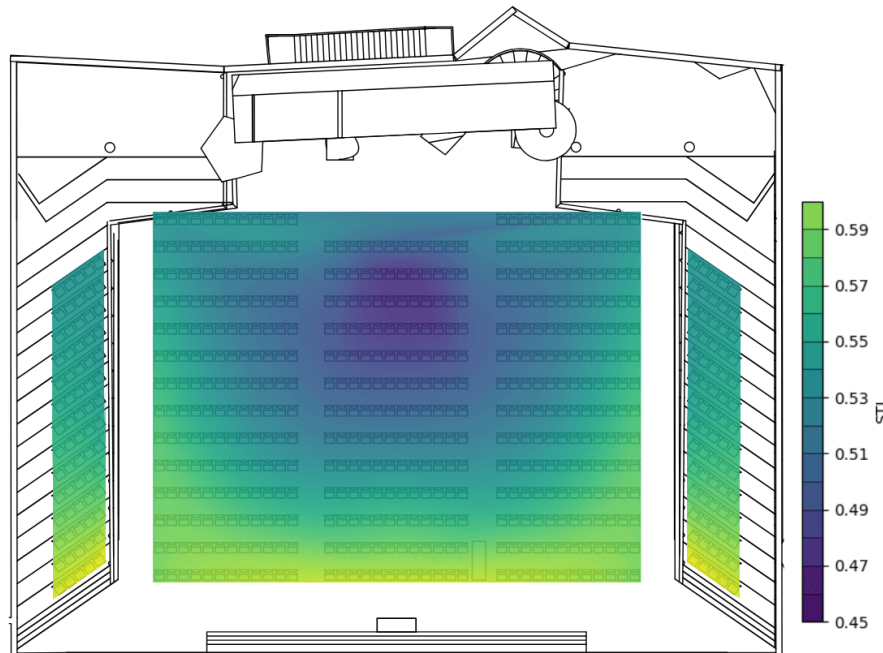


Figure 27: Speech Transmission Index spatial distribution.

5.5 Sound Strength G

In order to obtain the Strength parameter from the conducted measurements, it is required to perform an impulse response measurement of the source in a free field at a distance of 10 m. Since

this measurement was not performed, the IR obtained from the second microphone position, which is approximately 10 meters from the source, was used as a reference.

This means that the Figure 28 does not strictly show the spatial distribution of the G parameter, but instead a relative comparison between the impulse response amplitude obtained across the 14 microphone positions.

As expected, the lower values can be found in the back rows. The front lateral seats show a 6 dB increase from the reference position, while the center front row only show a 4 dB increase. This can be explained by the contribution of the reflections from the side walls.

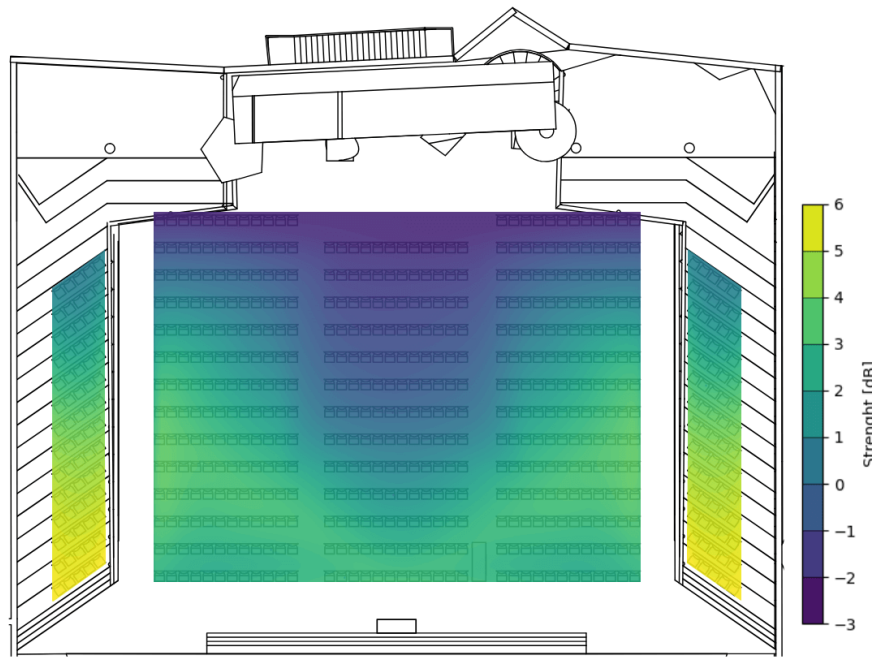


Figure 28: Strength spatial distribution for 1 kHz.

5.6 Lateral Fraction (LF)

Figure 29 shows the Lateral Fraction parameter by third octave bands.

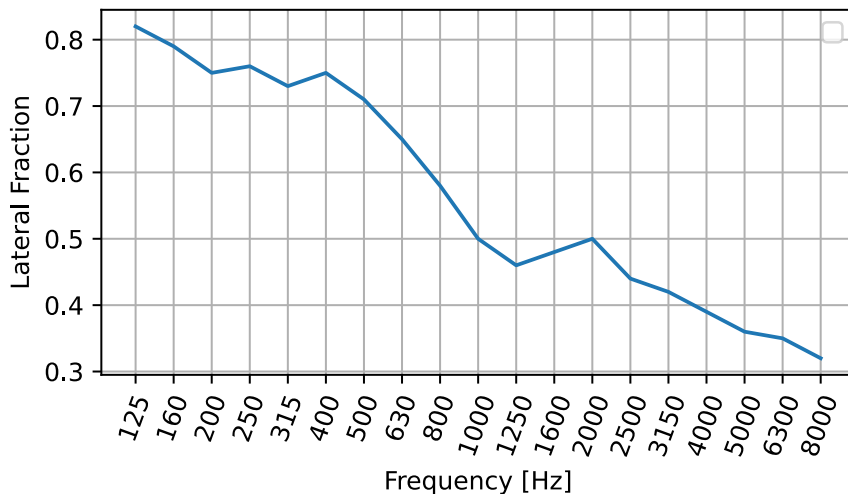


Figure 29: Lateral fraction.

The average values range from 0.05 for the 8 kHz band to 0.8 for the 160 Hz band. The larger the magnitude of the lateral fraction, the more lateral energy will be picked up at the microphone position, implying that the audience may interpret the lower frequency range as more spacious or enveloping. Instruments such as double bass, bassoon or trombone may sound enveloping to the audience, while instruments such as flute, oboe or soprano may be perceived as more direct. Judging by this parameter, it can be concluded that the auditorium is not suitable for chamber or symphonic music.

Figure 30 and 31 shows the Lateral Fraction (L_{50} and L_{80}) obtained from the subjective RIRs for 10, 100 and 350 ms.

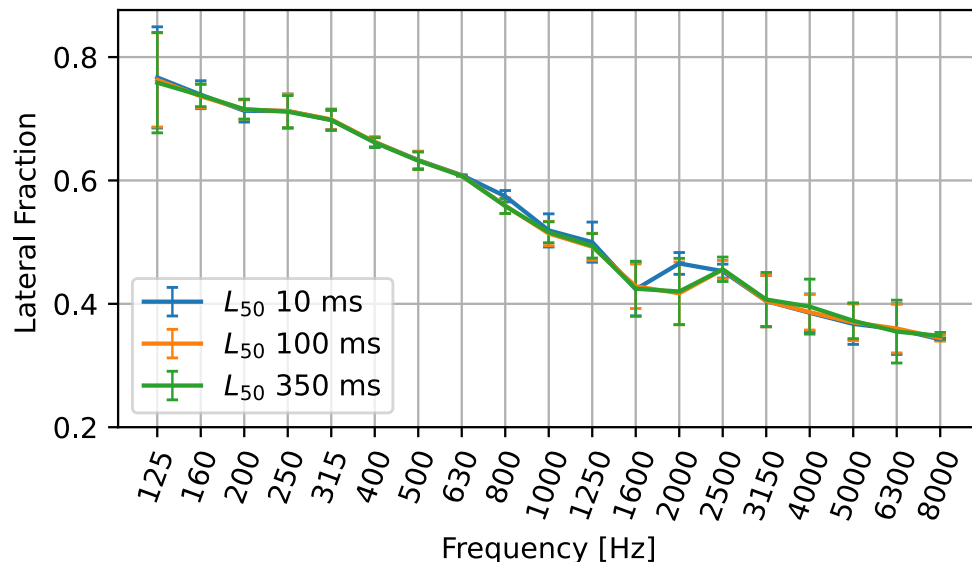


Figure 30: L_{50} values with different integration times.

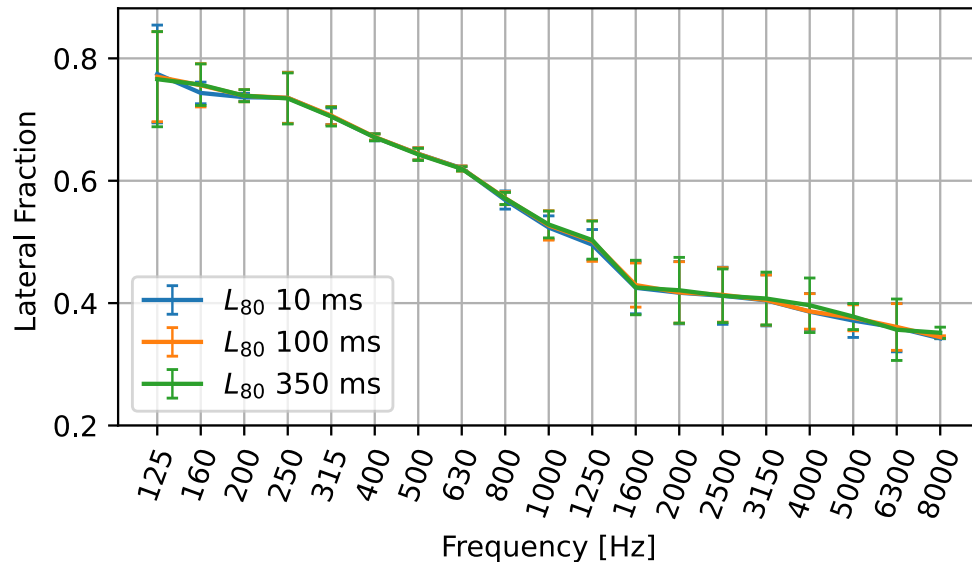


Figure 31: L_{80} values with different integration times.

Figure 30 and 31 reveals that the lateral fraction decreases with increasing frequency for the three delay times studied (10 ms, 100 ms and 350 ms). The side fraction is higher at lower frequencies,

with mean values ranging from 0.8 for the 160 Hz band to 0.3 for the 8 kHz band. This suggests that the higher the magnitude of the side fraction, the more lateral energy will be picked up at the microphone position. As a result, the audience may perceive the lower frequencies as more spacious or enveloping.

5.7 D/R

Figure 32 shows the average D/R value for each microphone.

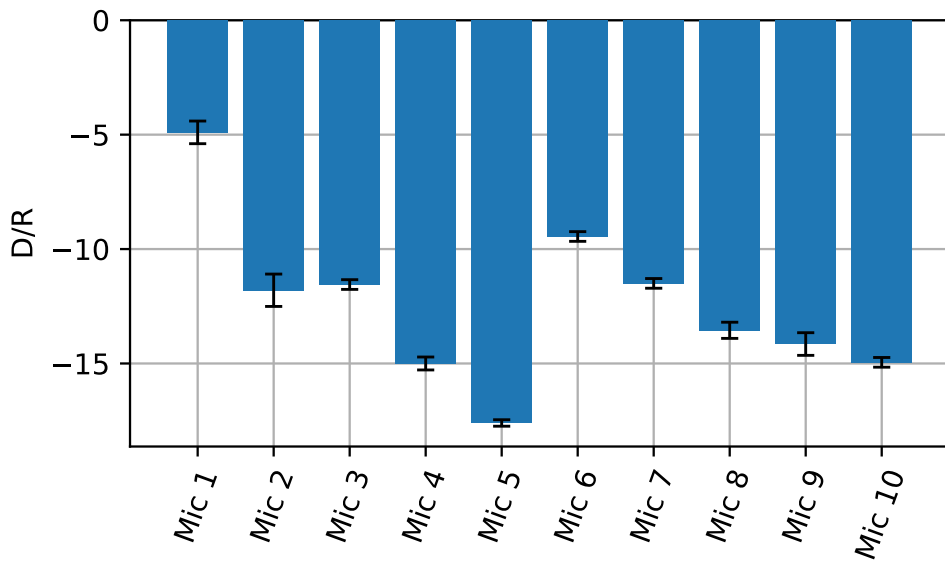


Figure 32: Direct to reverberant ratio measured in the main seating area.

The Figure 32 shows that microphones 1 and 5 receive more energy than the rest of the microphones. The measurement results of microphone 6 are remarkably interesting, as they show a higher D/R than the surrounding seats. This disparity could be attributed to the fact that this seat is located at the edge of the stalls, possibly acting as a diffuser, mitigating reflections coming from the ceiling.

In addition, a significant deviation is observed in all values. This variation could be due to inherent errors in the measurements, such as fluctuations in the source level between each sound recording stage.

The spatial distribution of D/R in the soil can be seen in Figure 33.

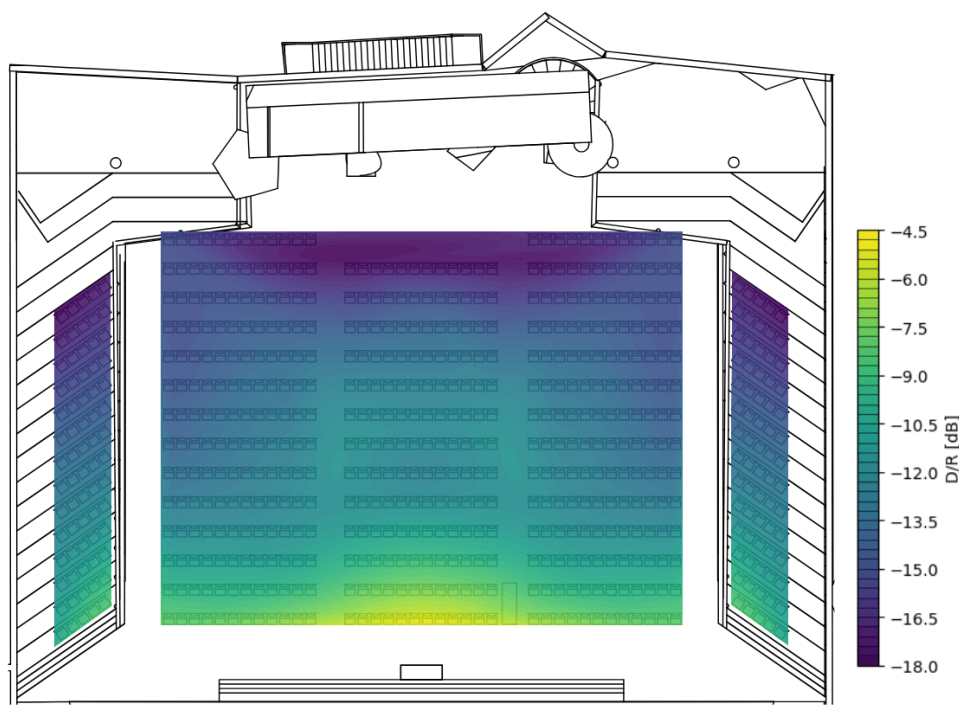


Figure 33: Direct to reverberant ratio spatial distribution.

It can be observed that, as the measuring point moves away from the sound source, the influence of the reverberant field increases.

When applying the 10, 100 and 350 ms subjective integration intervals, the average D/R value are 9.15 dB, 9.10 dB and 8.85 dB, respectively. Looking at Figure 33, it can be perceived that these values are very similar to the D/R values corresponding to the objective map.

5.8 IACC and LEV

The IACC parameter was calculated from the binaural measurements made with the KEMAR. Figure 34 shows the results of the two Kemar positions (P1 and P2) combined with the three source positions (S1, S2 and S3, being S1 the center position, S2 right side of the stage and S3 left side of the stage).

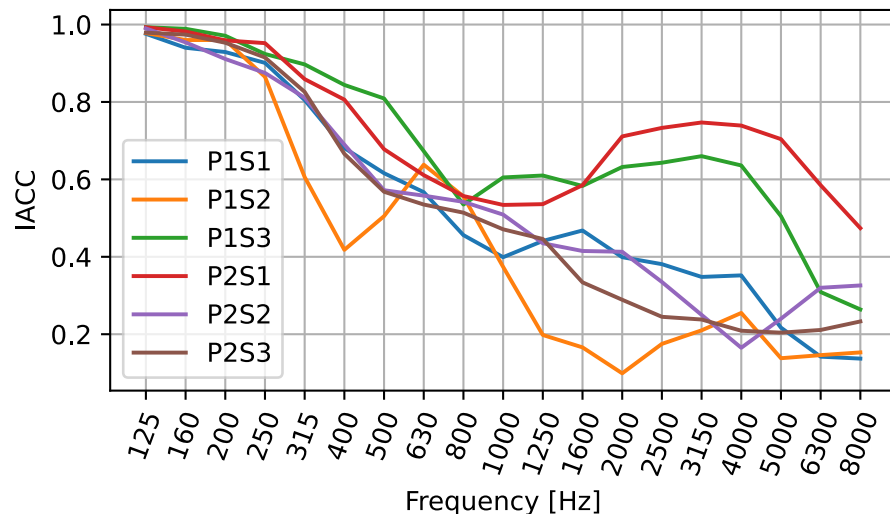


Figure 34: Interaural Cross-correlation for six Kemar positions.

It is observed that the IACC of the mid and high frequencies falls within Beranek's recommended values, which range from "good" to "excellent" [14]. This indicates that listeners should not experience difficulty in locating sound sources whose frequencies are above 500 Hz. It should be noted that the decrease in the IACC as frequencies increase is an expected phenomenon, since, in this range, the wavelength is negligible compared to the dimensions of the KEMAR head, resulting in a very low correlation between the signals picked up by each capsule.

On the contrary, in the case of low frequencies, where the wavelength is considerably larger than the head size, a maximum correlation between binaural signals is observed.

The positions that show a higher IACC are P2S1 and P1S3. This is due to the Kemar being placed right in front of the source, whereas the position P1S2 shows the lower IACC because the Kemar is placed in the left side of the audience area and the source is at the right side of the stage.

The mean value of the listening development measure (LEV) stands at 5.35 with a standard deviation of ± 0.30 . According to the references provided by Beranek [27], this auditory is not particularly distinguished for generating an extreme sensation of sound immersion, suggesting that the perception of being surrounded by sound is not notably intense in this specific space.

5.9 ACF and τ_e

Table 6 shows both the mean τ_e and the minimum τ_e with 95 % percentile for the different anechoic signals used for the enclosure evaluation.

Table 6: τ_e corresponding to each reproduced anechoic signal.

Audio	Minimum τ_e [ms]	Average τ_e [ms]
Clarinet	230,9	926,2
Electronic Drums	4,1	14,9
Voice	37,2	103,3

Signals with higher τ_e values are characterized by slower and more monotonous signals. This type of signal results in a long integration window in the ear, which can attenuate or mask immediate acoustic phenomena. Both the clarinet signal and the voice signal, used for the study of the room, have this attribute. These signals can complicate the acoustic appreciation of a room, unless an abrupt interruption occurs, which again alters the integration window of our ears.

Figure 35 shows the behaviour of the minimum τ_e (figure 35(a)) and the average τ_e (figure 35(b)) corresponding to the anechoic signal of the clarinet over the area of the auditorium.

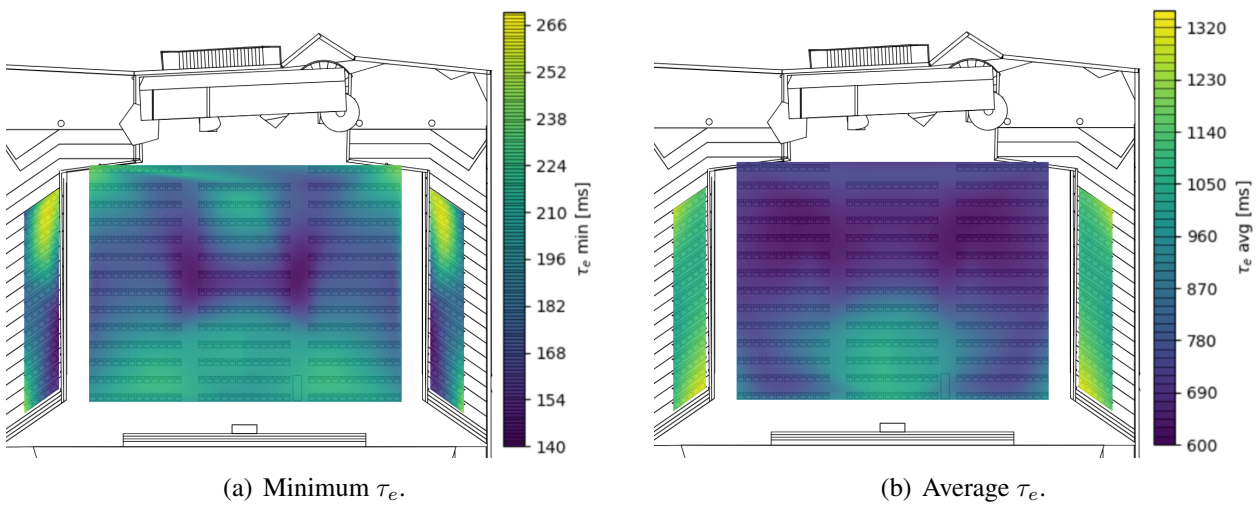


Figure 35: Anechoic clarinet audio.

It is noticeable that, despite being a signal whose τ_e is relatively long, the room made modifications. In the case of the minimum τ_e , an average modification of 24 % was obtained, although in some positions there were even alterations of 57 %, especially in the rear positions of the side balconies. On the other hand, although, on average, the average tau alteration was around 19 % in general, in the positions closest to the side balcony stage, this modification reached up to 42 %.

Figure 36 shows the parameter variations in the room, corresponding to the anechoic voice signal.

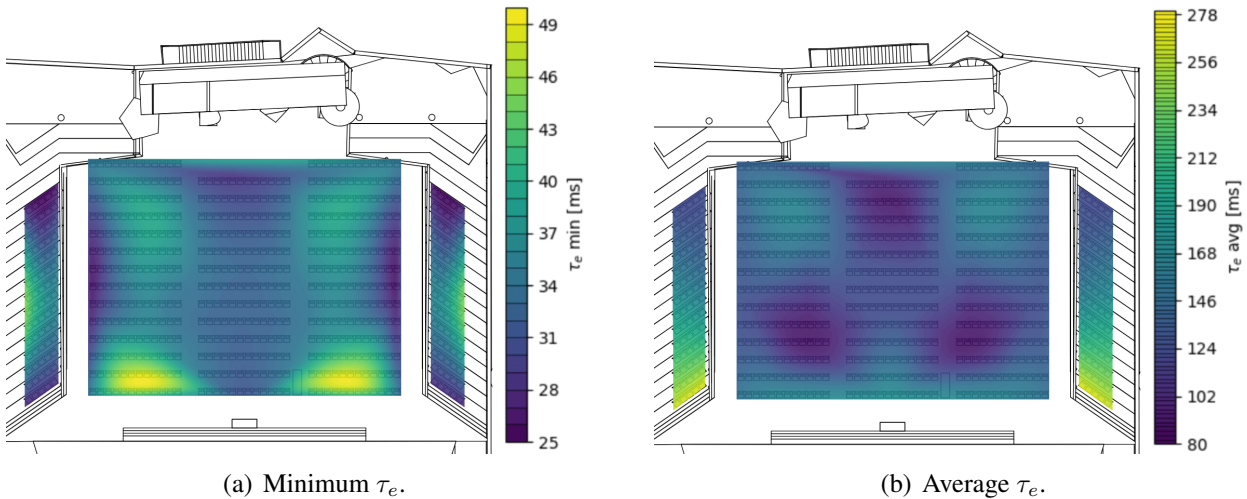


Figure 36: Anechoic voice audio.

The room changed the minimum τ_e by an average of 22 %, while the average τ_e changed by an average of 44 %. The largest change in minimum τ_e occurred at the rear of the central audience, reaching 48 %, while the maximum change of 170 % in average τ_e occurred at the rear of the side balconies.

Figure 37 shows the behaviour of the parameters of the anechoic signal of the drums across the length and width of the enclosure.

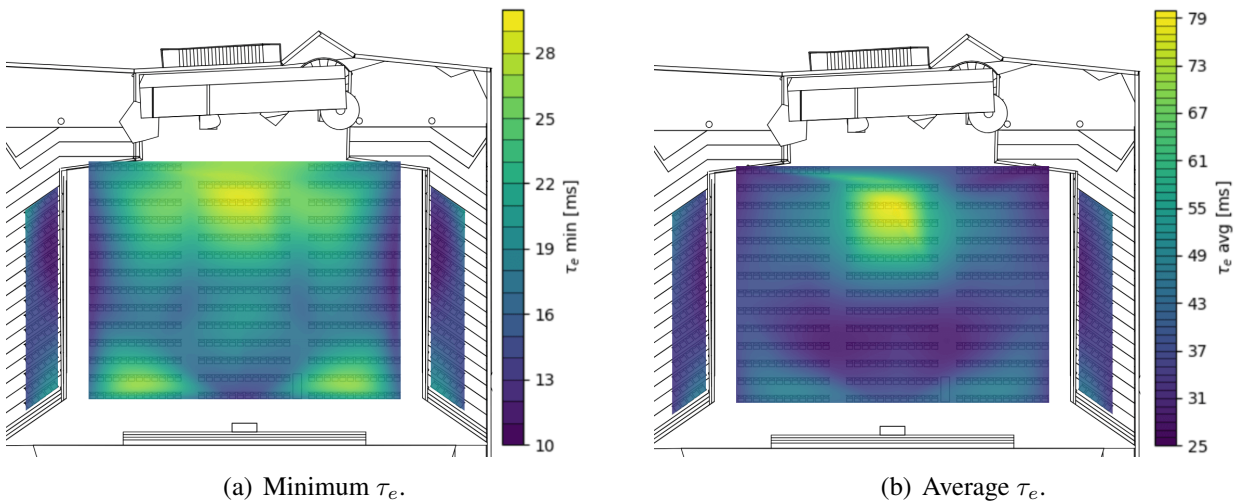


Figure 37: Anechoic electronic drums audio.

The τ_e of the drum signal changed the most due to the room: the minimum τ_e changed by 359 % on average, while the average τ_e changed by 177 % on average. The maximum room intervention in the minimum τ_e was in the front area of the audience, very close to the stage, in the central area where it touched 604 %. Here, also, is where the maximum variation of the average τ is noted, reaching 426 %.

5.10 Centre Time (TS)

In the Figure 38, an average of $58 \text{ ms} \pm 10 \text{ ms}$ is observed in the lower level and $163.1 \text{ ms} \pm 9.8 \text{ ms}$ in the upper level. It is observed that these values increase primarily with the distance from the stage. This trend indicates that the stochastic part of the impulse response has greater energy than the deterministic component, resulting in a modification of the impulse response's center of gravity.

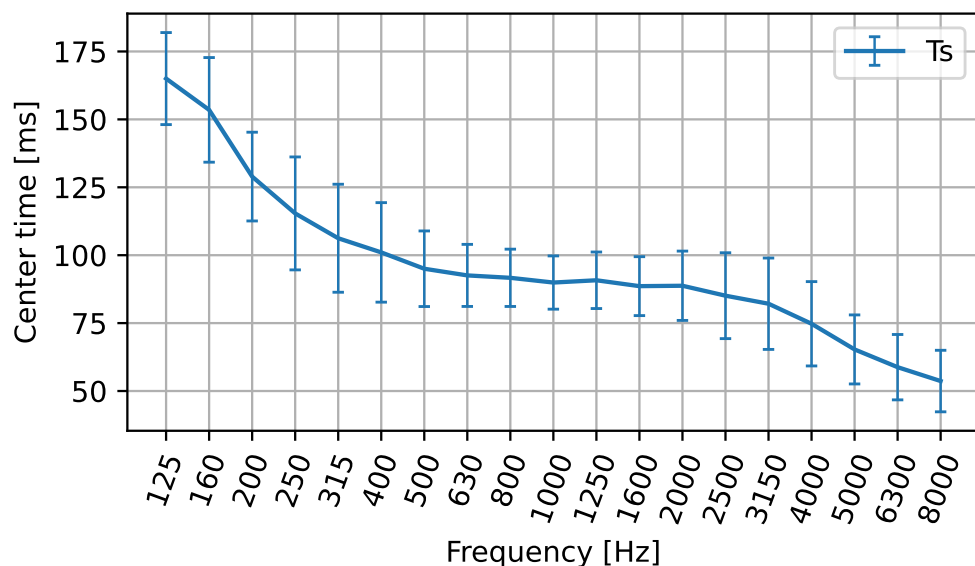


Figure 38: Average Ts value over the entire audience area.

Another way to interpret this phenomenon is by analyzing the first reflections and how these are

fainter at the more distant seats. Figure 42 illustrates the spectral distribution of the Ts of the different zones as a function of frequency. Also, the central times of the different Reverberation Impulse Responses (RIR) in the audience area are presented in Figure 39, 40 and 41.

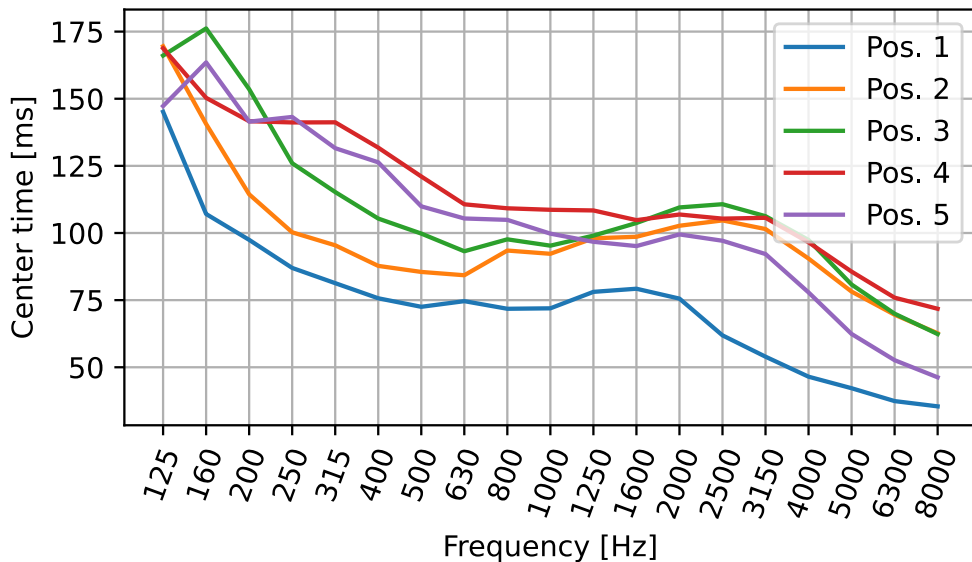


Figure 39: Ts values from position 1 to 5 of audience.

In the Figure 39, it is observed that in the first five rows, the TS curve in the first position is lower than the other curves, being the curve of the fourth position higher, this is due to the fact that the first reflections are weaker for the farthest seats. On the other hand, the fifth position of the microphone is not the highest Ts curve, this may be due to the fact that the microphone is close to the stalls walls.

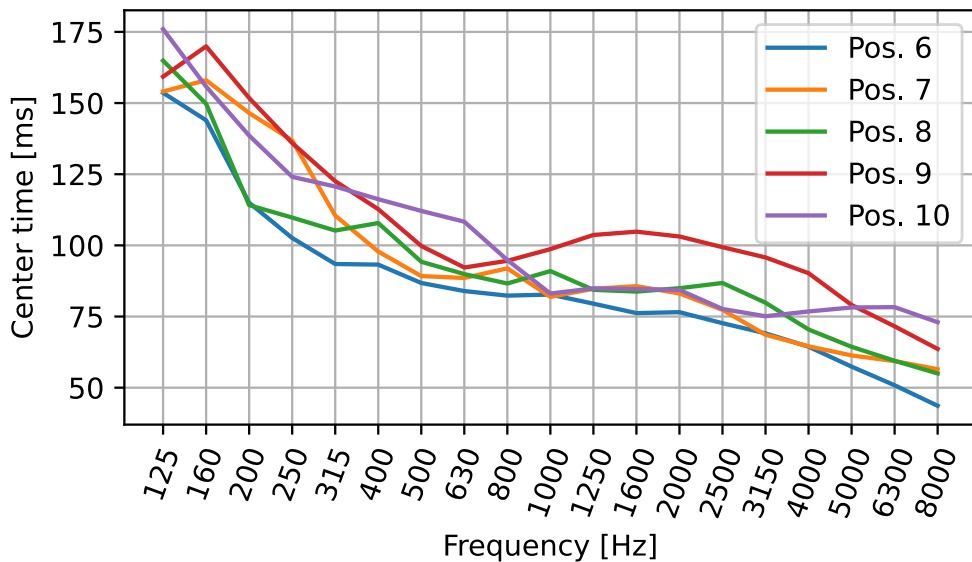


Figure 40: Ts values from position 6 to 10 of audience.

In the Figure 40, it can be observed that in the second five positions. In this case, the situation is similar to the previous one, the TS curve in the sixth position is lower than the other curves, with the curve of the ninth position being the highest. Again, the tenth microphone position is not the curve

with the highest Ts, this may be because the microphone is located near the walls of the stands, thus receiving early reflections with higher energy compared to the microphone in the ninth position.

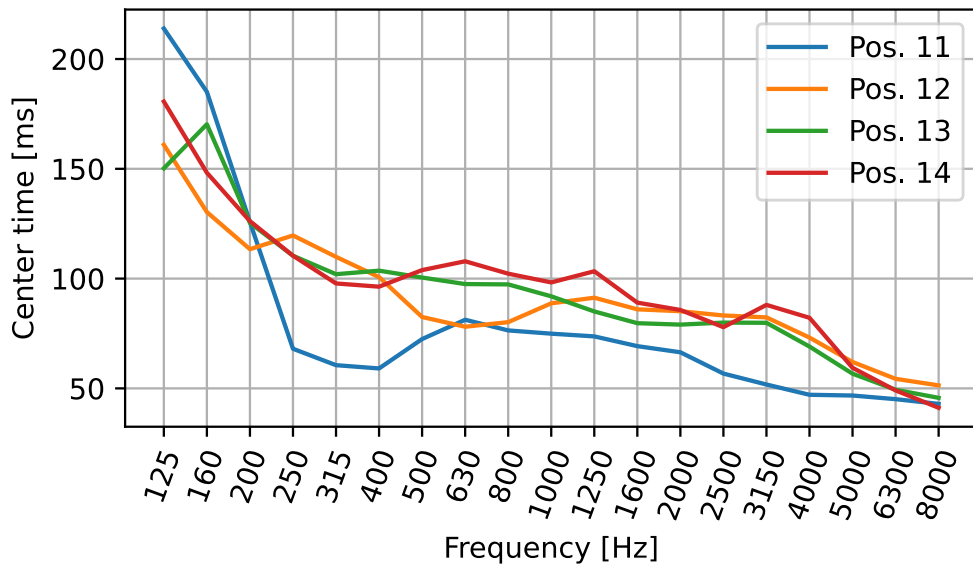


Figure 41: Ts values from position 11 to 14 of audience.

Finally, in the Figure 41, it is observed that the eleventh position has the lowest curve compared to the fourteenth position, which has the highest curve. This contrasts with the position of the microphones furthest from the measurement source.

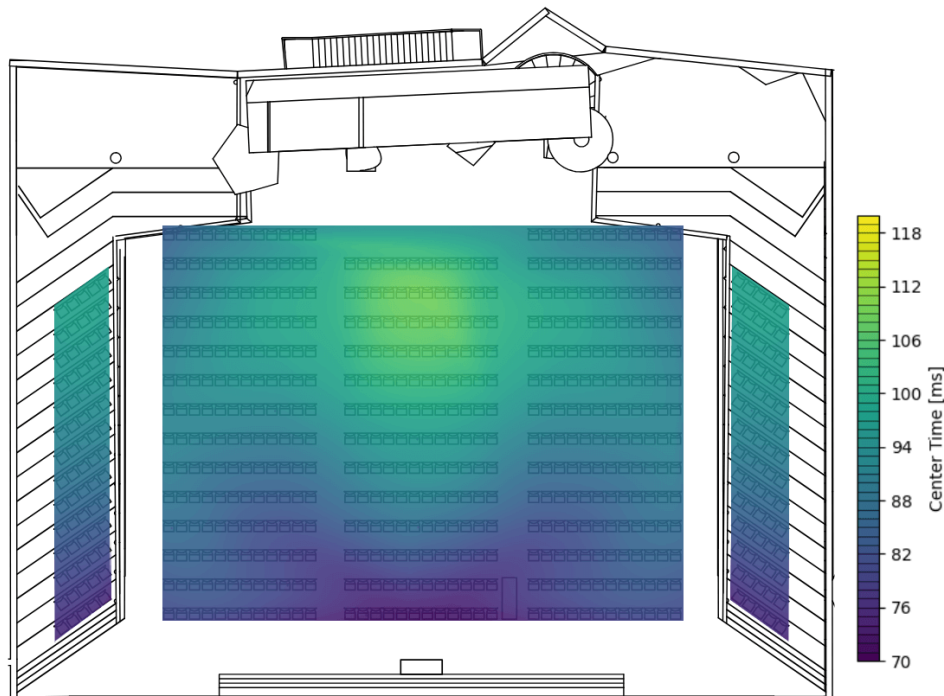


Figure 42: Spatial distribution of the center time.

In the Figure 42, what was mentioned above can be observed, where it can be seen that the greater the distance from the source, the greater the Ts will be because the first reflections will be lower. Therefore, the last seats relative to the stage will have fewer primary reflections.

5.11 Stage parameters

ISO 3382-1 specifies that the ST_{early} and ST_{late} Support values are determined as the average of octave frequency bands ranging from 250 Hz to 2 kHz. These values provide a unique measure to quantify and evaluate the discrepancy between two specific sound levels: the direct sound in comparison to the early sound, as well as the direct sound in relation to the late sound. From the measurements it appears that:

$$ST_{early} = -9,961 \text{ dB} ; ST_{late} = -8,710 \text{ dB}$$

The values are negative due to the microphone-sound source measurement distance; at 1 m, there is more active field than reactive field.

According to the reference values proposed by Gade, the resulting ST_{early} measurement indicates that the studio auditorium is optimal for chamber music performance. However, it is important to note that this space is used for oral speeches as well as shows. In this context, Bistafa recommends a slightly higher value, specifically 0.461 dB above the value measured in the hall.

On the other hand, it is relevant to note that the measured value of ST_{late} in the auditorium is outside the typical range between -24 dB and -10 dB . Specifically, this value is 1.29 dB above the upper limit of the established range. This result suggests a more pronounced presence of late sounds relative to the direct sound, denoting the degree to which the room supports the musicians through reflections (room response).

5.12 Echo Speech and Echo Music

The results obtained are shown in Figure 43 for the Echo Speech and in Figure 44 for the Echo music.

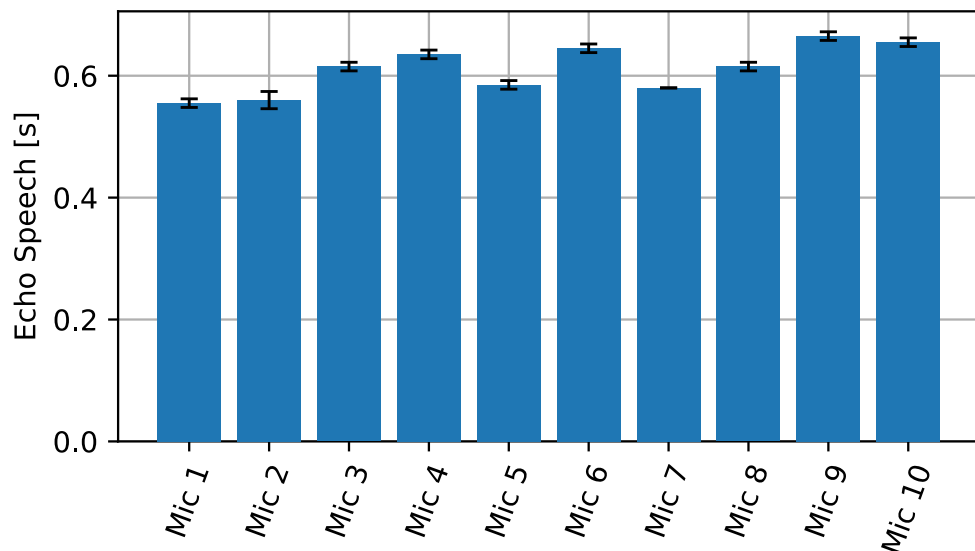


Figure 43: Echo speech measured in the main seating area.

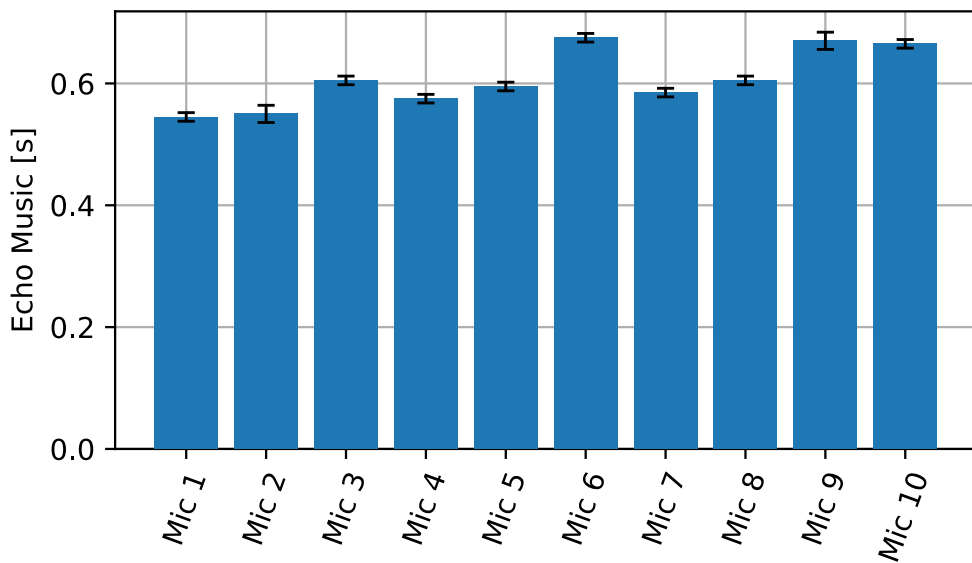


Figure 44: Echo music measured in the main seating area.

Both parameters are below the technical threshold, even considering its most stringent value (EK[10%]), which applies to people with years of auditory training. As detailed in Table 5, the maximum tolerated values for this condition are 0.9 for EchoSpeech and 1.5 for EchoMusic. This indicates that listeners will not perceive the reflections as an annoying echo, regardless of the level of auditory training or the type of content presented (speech or music).

The values obtained range from 0.5 to 0.7, suggesting that there should be no echo problems in any of the seating positions evaluated. Furthermore, both parameters were calculated using the same integration windows that were used for the EDT calculation: 10, 100 and 350 ms, in order to evaluate them subjectively. The average Echo Speech value for each integration window is 0.84 s, 0.82 s and 0.81 s, respectively. For the Echo Music parameter, the values are 0.72 s for every integration window.

It is observed that in all cases, the subjective values are higher than the objective values, and the same is true for the uncertainty values. Specifically, for both parameters, the maximum value was found in the 10 ms integration window, suggesting a higher probability that impulsive sounds are perceived as echoes, in agreement with common sense. However, all values remain below the annoyance threshold, indicating that, in principle, the echo does not represent a significant problem.

6. Conclusion

This study presents a comprehensive acoustic analysis of Auditorio de la Paz at Soka Gakkai, located in Capital Federal, Argentina. The evaluation included diverse acoustic parameters derived from extensive measurements and analyses using various recording techniques, such as monophonic recordings with omnidirectional microphones, binaural recordings with a KEMAR, and Ambisonics recordings with a Soundfield microphone. The primary source for analysis was an omnidirectional source (dodecahedron), supplemented by assessments using a two-way loudspeaker to gauge intelligibility.

The results revealed that the reverberation times (T20 and T30) in the mid and high frequencies closely matched expected values for a multipurpose hall of similar volume. This suggests favorable acoustic conditions for various events, maintaining clarity and avoiding excessive reverberation that could compromise intelligibility. The auditorium demonstrated effective control of early reflections, with consistent EDT values across the frequency spectrum and a relatively uniform spatial distribution in the listening area, although some uncertainty persisted at lower frequencies.

Parameters crucial for speech intelligibility, such as C50 and STI, indicated optimal conditions for spoken word events, ensuring clear articulation and good audibility throughout the auditorium. However, challenges were noted with C50 values, particularly affecting comprehension in certain seating positions and frequency bands, suggesting potential improvements in these areas.

In terms of musical performance, the auditorium exhibited acceptable clarity (C80), indicating suitable conditions for musical events. Nonetheless, further enhancements in specific frequency bands could improve overall musical intelligibility and audience experience.

The assessment of lateral sound information, including IACC values for mid and high frequencies, suggested that listeners would have no difficulty locating sound sources within this range. However, the presence of significant lateral reflections at specific positions, as indicated by JLF results, highlighted potential areas for acoustic refinement.

The Strength parameter (G) demonstrated generally optimal values for both musical and speech purposes, though significant uncertainty in its calculation suggested a non-uniform distribution throughout the auditorium.

Echo parameters met acceptable standards across the auditorium, indicating that reflections would not be perceived as an annoying echo by listeners, regardless of their auditory training or the content presented (speech or music). Subjective analysis of these parameters found values below the annoyance threshold, confirming a positive acoustic environment.

In relation to LF, it is noted that as the magnitude of the lateral fraction increases, more lateral energy will be picked up at the microphone position, suggesting that the audience may perceive the lower frequency range as more spacious or enveloping. Instruments such as double bass, bassoon or trombone may sound enveloping to the audience, while instruments such as flute, oboe or soprano may be perceived as more direct. Therefore, this parameter indicates that the auditorium is not suitable for chamber or symphonic music. On the other hand, the LEV indicates that it is not particularly distinguished by sound immersion, suggesting that the perception of being surrounded by sound is not particularly intense in this specific space.

Finally, the center time analysis indicated that greater distances from the source resulted in lower energy from first reflections, influencing the auditorium's spatial acoustics.

Some recommendations for enhancing acoustic performance included the installation of acoustic clouds or panels on the ceiling to reduce overhead sound reflections, thereby improving clarity parameters such as C50 and reducing reverberation times, consequently enhancing the EDT. Additionally, optimizing seating with higher absorption coefficients was proposed to promote a more uniform sound field, further reducing EDT and improving overall clarity.

A proposal to design low-frequency diffusers for the side walls, particularly those adjacent to balconies, aimed to address variations in reverberation times within this range, ensuring a more balanced acoustic environment throughout the auditorium.

In conclusion, Auditorio de la Paz at Soka Gakkai exhibits generally favorable acoustic characteristics suitable for a variety of events, including both musical performances and speech presentations. While the auditorium's design leans slightly more towards optimal conditions for speech, improvements in targeted acoustic treatments and seating modifications could enhance its versatility and acoustic performance, ensuring an enriched auditory experience for all attendees.

References

1. ISO 3382-1:2009. Acoustics — measurement of room acoustic parameters — part 1: Performance spaces. Standard, International Organization for Standardization, Geneva, CH, 2009.
2. Wallace Clement Sabine. Collected papers on acoustics: Paper 1—reverberation. 1922.
3. Vilhelm Lassen Jordan. Acoustical criteria for auditoriums and their relation to model techniques. *Journal of the Acoustical Society of America*, 47:408–412, 1970.
4. O. Abdel-Alim. Dependence of time and register definition of room acoustical parameters with music performances. *Dresden: TU Dresden*, 1973.
5. M. R. Schroeder, D. Gottlob, and K. F. Siebrasse. Comparative study of European concert halls: correlation of subjective preference with geometric and acoustic parameters. *The Journal of the Acoustical Society of America*, 56(4):1195–1201, 10 1974.
6. Matthew G. Blevins, Adam T. Buck, Zhao Peng, and Lily M. Wang. Quantifying the just noticeable difference of reverberation time with band-limited noise centered around 1000 hz using a transformed up-down adaptive method. 2013.
7. Jukka Pätynen, Brian F.G. Katz, and Tapio Lokki. Investigations on the balloon as an impulse source. *The Journal of the Acoustical Society of America*, 129(1):EL27–EL33, 01 2011.
8. Marko Horvat, Kristian Jambrošić, and Hrvoje Domitrović. A comparison of impulse-like sources to be used in reverberation time measurements. *The Journal of the Acoustical Society of America*, 123:3501, 06 2008.
9. Dragana Pavlović, Miomir Mijic, and Husnija Kurtovic. A simple impulse sound source for measurements in room acoustics. *Applied Acoustics - APPL ACOUST*, 69:378–383, 04 2008.
10. Angelo Farina. Simultaneous measurement of impulse response and distortion with a swept-sine technique. 11 2000.
11. Angelo Farina. Advancements in impulse response measurements by sine sweeps. *Journal of The Audio Engineering Society*, 2007.
12. Angelo Farina. Auralization software for the evaluation of the results obtained by a pyramid tracing code: Results of subjective listening tests. 2000.
13. P. Brown. Easera-a powerful audio and acoustic testing platform. *Syn-Aud-Con Newsletter*, 32:2, 2005.
14. Leo Leroy Beranek. *Concert halls and opera houses: music, acoustics, and architecture*, volume 2. Springer, 2004.
15. Roberto Daniel Ottobre, Marcelo Ottobre, Agustín Arias, and Guadalupe Cuello. Acoustics of the Border Cultural Centre in the neighbourhood of Palermo, city of Buenos Aires, Argentina. *Proceedings of Meetings on Acoustics*, 28(1):015026, 06 2017.
16. Gustavo Basso. Acoustics of the Blue Whale Auditorium in Buenos Aires. *Building Acoustics*, 28(3):209–230, 2021.
17. Ernesto Accolti, Yesica Alamino Naranjo, Alción Alonso Frank, and Ernesto Kuchen. The acoustics of the concert hall Auditorio Juan Victoria from San Juan, Argentina. *Proceedings of Meetings on Acoustics*, 28(1), 09 2016.
18. Simone Campanini, Angelo Farina, et al. *A new audicity feature: room objective acoustical parameters calculation module*. na, 2009.
19. IEC 60268-16:2020. Sound system equipment - part 16: Objective rating of speech intelligibility by speech transmission index. Standard, International Electrotechnical Commission, 2020.

20. VMA Peutz. Articulation loss of consonants as a criterion for speech transmission in rooms. In *Audio Engineering Society Convention 2ce*. Audio Engineering Society, 1972.
21. Michael Barron and Arthur Harold Marshall. Spatial impression due to early lateral reflections in concert halls: the derivation of a physical measure. *Journal of sound and Vibration*, 77(2):211–232, 1981.
22. M. Morimoto. The role of rear loudspeakers in spatial impression. In *Audio Engineering Society Convention 103*, 98, 9 1997.
23. Soulodre G. A. and Bradley J. S. Subjective evaluation of new room acoustic measures. *The Journal of the Acoustical Society of America*, 98:294–301, 1995.
24. Akiko Wakuda, Hiroshi Furuya, Kazutoshi Fujimoto, Kenji Isogai, and Ken Anai. Effects of arrival direction of late sound on listener envelopment. *Acoustical Science and Technology*, 24, 07 2003.
25. David Griesinger. The psychoacoustics of apparent source width, spaciousness and envelopment in performance spaces. *Acta Acustica united with Acustica*, 83:721–731, 07 1997.
26. D. Nyberg. Listener envelopment: effects of changing the sidewall material in a model of an existing concert hall. *Luleå University of Technology*, 2008.
27. Leo Leroy Beranek. Listener envelopment lev, strength g and reverberation time rt in concert halls. 2010.
28. Yoichi Ando and Daniel R Raichel. Architectural acoustics: blending sound sources, sound fields, and listeners. 1998.
29. Anders Gade. Investigations of musician's room acoustics conditions in concert halls, part ii. *Acta Acustica united with Acustica*, 69:249–262, 01 1989.
30. L. Jr and Sylvio Bistafa. Evaluation of stage acoustics of two multipurpose auditoriums in São Paulo by measuring stage support, st1. *International Congress on Noise Control Engineering 2005, INTERNOISE 2005*, 4:3257–3266, 01 2005.
31. L. Dietsch and W. Kraak. Ein objektives Kriterium zur Erfassung von Echostörungen bei Musik- und Sprachdarbietungen. *Acta Acustica United with Acustica*, 60(3):205–216, 1986.
32. Ahmed Ali Elkhateeb. The acoustical design of the new lecture auditorium, faculty of law, Ain Shams university. *Ain Shams Engineering Journal*, 3, 2012.
33. Heinrich Kuttruff. *Room acoustics*. CRC Press/Taylor & Francis Group, 2017.
34. Krzysztof Leo. Speech intelligibility measurements in auditorium. *Acta Physica Polonica A*, 118, 07 2010.
35. Michael Barron. Using the standard on objective measures for concert auditoria, ISO 3382, to give reliable results. *Acoustical Science and Technology*, 26:162–169, 2005.
36. J. S. Bradley. Predictors of speech intelligibility in rooms. *The Journal of the Acoustical Society of America*, 80(3):837–845, 09 1986.
37. Soka Gakkai. Localización del auditorio de la paz Soka Gakkai. <https://maps.app.goo.gl/Rt3cmWTrbiVgxpGH6>.
38. Tsunesaburō Makiguchi. https://es.wikipedia.org/wiki/Tsunesabur%C5%8D_Makiguchi, Jan 2024.
39. Jōsei Toda. https://es.wikipedia.org/wiki/J%C5%8Dsei_Toda, Dec 2023.
40. Daisaku Ikeda. https://es.wikipedia.org/wiki/Daisaku_Ikeda, Dec 2023.
41. Soka Gakkai. Historia de la Soka Gakkai. <https://www.sokaglobal.org/es/about-the-soka-gakkai/our-history.html>, Dec 2023.

42. Auditorio de la Paz Soka Gakkai Argentina. https://es.wikiarquitectura.com/edificio/auditorio-de-la-paz-soka-gakkai-argentina/auditorio-de-la-paz-clorindo-testa-buenos-aires-wikiarquitectura_028/.
43. Trevor Cox and Peter d'Antonio. *Acoustic absorbers and diffusers: theory, design and application*. CRC press, 2016.
44. Glen Ballou. *Handbook for sound engineers*. Taylor & Francis, 2013.

Preguntas

1. ¿Qué problemas acústicos presenta la sala medida?

- El parámetro EDT presenta valores similares en todo el espectro, y la distribución espacial en la zona de la audiencia era relativamente uniforme, aunque persistía cierto grado de incertidumbre en bajas frecuencias.
- Los valores de C50 sugieren que habrá problemas de comprensión de los disertantes, ya que no cumplen los valores recomendados dentro del rango habitual de la voz humana.

2. ¿Cómo mejoraría la acústica de la sala medida? (liste 3 actividades a realizar en orden de prioridad, de mayor efecto a menor efecto).

- El diseño e instalación de difusores y trampas de graves para tratar las bajas frecuencias es fundamental para mejorar el tiempo de decaimiento temprano (EDT). Tratar las frecuencias bajas, mediante la colocación de trampas de graves en las esquinas de la sala y difusores en las paredes laterales y traseras, ayuda a dispersar las ondas sonoras y evitar acumulaciones de energía en estas áreas. Esta estrategia reduce los picos de resonancia y mejora la uniformidad del tiempo de reverberación, resultando en una percepción de claridad y definición del sonido más equilibrada.
- La instalación de butacas con mayor coeficiente de absorción, favorece la uniformidad del campo sonoro, reduce el EDT y favorece el parámetro de claridad C50.
- La colocación estratégica de nubes acústicas o paneles absorbentes de baja frecuencia en el techo puede ser una intervención significativa para mejorar el tiempo de decaimiento temprano (EDT). Aunque tradicionalmente se utilizan para tratar frecuencias medias y altas, los paneles diseñados específicamente para bajas frecuencias pueden contribuir eficazmente a la reducción del EDT. Utilizar paneles de baja frecuencia o nubes acústicas con materiales que absorban eficazmente estas frecuencias y colocarlos en zonas estratégicas del techo donde las reflexiones son más problemáticas permite controlar la propagación del sonido desde arriba. Esto reduce las reflexiones de bajas frecuencias y, en consecuencia, mejora tanto el EDT como la claridad del sonido.

3. ¿Cómo relacionaría la inteligibilidad de la fuente con la variación del τ_e que produce la sala en cada posición?

Al comparar los valores obtenidos de los parámetros de inteligibilidad (STI y ALCons%) con la variación de τ_e , se puede observar que a lo largo de las posiciones medidas, los valores de inteligibilidad permanecen relativamente constantes en un rango medio. De manera similar, la variación de τ_e también se mantiene constante a lo largo de estas posiciones.

En los puntos extremos donde el STI alcanza valores mínimos, se percibe un leve aumento en la variación de τ_e . Por lo tanto, se podría considerar que ambos parámetros son inversamente proporcionales. No obstante, un análisis más detallado de la relación entre ambos parámetros requeriría una mayor variación en ambos para permitir una evaluación más precisa.